Supplementary Information to “Use of a mechanistic physiologically based kinetic model and quantitative in vitro to in vivo extrapolation to evaluate the tolerable daily intake of zearalenone”

Chrysanthi Pachoulide[1,*], Joost Westerhout [2], Hans Bouwmeester[1] and Nynke I. Kramer[1]
[1]Division of Toxicology, Wageningen University and Research, The Netherlands
[2]The Netherlands and 2Center for Prevention, Lifestyle and Health, National Institute for Public Health and the Environment (RIVM), The Netherlands

Table S1: Current knowledge of the toxicokinetic processes determining the fate of ZEN and its most prominent metabolites in humans and rats, based on in vitro and in vivo studies.

Method	Results	Reference
	Absorption	
Intestinal perfusion of an isotonic solution of ZEN at 4 µg/ml; in Wistar rats (6 males).	***ZEN:*** • **ka:** 9.27(0.69) /h • Intestinal absorption fits first order kinetics • Complete intestinal absorption via passive diffusion	(Ramos et al., 1996)
Exposure to 10 µM ZEN on the mucosal side of the everted small (excluding duodenum) and large intestine of Sprague-Dawley rats (6 males (m); 6 females (f); 6 pregnant females (pf))	***ZEN:*** • Disappearance rate from the mucosal side: (m) 200, (f) 100, (pf) 70 nmol /10cm intestine /h • The rate decreased in the distal small intestine of males and pregnant females ***α-ZEL:*** Not detected; completely metabolised to α-ZEL GlcA	(Ieko et al., 2020)
Exposure to 10 µM and 200 µM ZEN on the apical (AP-BL) and basolateral side (BL-AP) of a Caco-2 cell monolayer for 8h.	***ZEN:*** • **Papp AP-BL:** (10 µM ZEN) 368(43), (200 µM ZEN) 2749(228) pmol/cm2/h • **Papp BL-AP**: (10 µM ZEN) 137(37), (200 µM ZEN) 2020(184) pmol/cm2/h • Intestinal absorption via passive diffusion • Apparent permeability decreased after 4h of exposure; due to extensive metabolism	(Videmann et al., 2008)
Exposure to 20 µM ZEN or α-ZEL on the apical side (AP-BL) of a Caco-2 cell monolayer for 1h.	***ZEN:*** • **Papp AP-BL:** 10.4(4.7) × 10-6 cm/s • *α-ZEL:* • **Papp AP-BL**: 5.4(0.5) × 10-6 cm/s	(Pfeiffer et al., 2011)
	Bioavailability	
Single IV bolus and PO administration of 1-8 mg/kg ZEN in intact and bile-duct cannulated male Sprague-Sawley rats (n=16). TK parameters were determined with non-compartmental analysis.	***ZEN:*** • **AUC, IV bolus:** 181(30), 335(107), 745(386) and 1696(481) ng h/ml at 1, 2, 4 and 8mg/kg ZEN • **AUC, PO:** 46.1(16.5) (intact), 19.3(0.3) (bile duct-cannulated) ng h/ml • **Fa:** (intact) 2.7, (bile duct cannulated) 1.1 %	(Shin et al., 2009)

Metabolism

	ZEN reduction	
Exposure to 40 µM ZEN on Caco-2 cells for 3h.	22 and 4 % reduced to α-ZEL and β-ZEL respectively	(Pfeiffer et al., 2011)
Exposure to 10 - 200 µM ZEN on the apical (AP-BL) side of a Caco-2 cell monolayer for 8h.	• Formation/secretion of *α-ZEL* followed Michaelis-Menten kinetics and was inhibited by 3α-HSD inhibitors • At low ZEN concentrations (<25 µM); secretion was higher in the AP-BL direction; at higher ZEN concentrations; secretion was higher in the BL-AP direction • α-ZEL was the main metabolite in the BL side and cells • Formation/secretion of *β-ZEL* was higher in the BL-AP direction; followed Michaelis-Menten kinetics and was inhibited by 3β-HSD inhibitors. • *β-ZEL* was mostly detected in the AP side.	(Ieko et al., 2020)
Incubation of rat S9 (post-mitochondrial) liver fractions with 10-2000 µM ZEN for 30 minutes.	***α-ZEL formation rate:*** • **liver microsomes:** 0.9 × 10-6 L/min/mg protein • **liver S9:** 0.05 × 10-6 L/min/mg protein • *β-ZEL formation rate:* • **liver microsomes:** 49.5 × 10-6 L/min/mg protein • **liver S9:** 3.43 × 10-6 L/min/mg protein	(Malekinejad et al., 2006)
Incubation of human microsomal or S9 liver fractions with 1-500 µM ZEN; for 10 and 5 minutes respectively.	***α-ZEL formation rate:*** • **liver microsomes:** 10.7 × 10-6 L/min/mg protein • **liver S9:** 38.7 × 10-6 L/min/mg protein	(Mendez-Catala et al., 2020)
Incubation of human and rat feces (5%; pH 7.4) with 1-250 µM ZEN for 5h.	***α-ZEL formation rate:*** • **Human feces:** 6.6 × 10-9 L/min/mg feces • **Rat feces:** 3.5 × 10-9 L/min/mg feces	
	Glucuronidation	
Exposure to 40 µM ZEN on Caco-2 cells for 3h.	• 11 % of ZEN metabolised to ZEN-GlcA • 14.8 % of *α-ZEL* metabolised to α-ZEL GlcA • 4.9 % of *β-ZEL* metabolised to β-ZEL GlcA	(Pfeiffer et al., 2011)
Exposure to 10 - 200 µM ZEN on the apical (AP-BL) side of a Caco-2 cell monolayer for 8h.	• α-ZEL GlcA was formed and secreted at a higher rate than ZEN GlcA • There was no formation of β-ZEL GlcA. • GlcA secretion was saturated and inhibited at high ZEN concentrations.	(Videmann et al., 2008)

	• GlcAs were mostly excreted in the AP side; undetectable in the cells.	
Exposure to 40 μM ZEN on Caco-2 cells for 3h.	14-O-GlcAs were the 97, 89 and 67 % of the total GlcAs formed for ZEN, α-ZEL and β-ZEL respectively.	(Pfeiffer et al., 2011)
Incubation of rat S9 (post-mitochondrial) liver fractions with 10-2000 μM ZEN for 30 minutes.	The % of Glucuronidation decreased from 89(2.7) to 12(5.0) with an increasing concentration of ZEN (10 to 250 μM)	(Malekinejad et al., 2006)
Incubation of human and rat S9 fractions with 0.3-150 μM ZEN or α-ZEL; for 7(liver) and 20(intestine) minutes respectively.	***ZEN-GlcA formation rate:*** • **Human liver S9:** 1.45 × 10-3 L/min/mg protein • **Human intestinal S9**: 0.42 × 10-3 L/min/mg protein • **Rat liver S9:** 1.04 × 10-3 L/min/mg protein • α-ZEL-*GlcA formation rate:* • **Human liver S9:** 1.24 × 10-3 L/min/mg protein • **Rat liver S9:** 1.24 × 10-3 L/min/mg protein	(Mendez-Catala et al., 2021)
Exposure to 10 μM ZEN on the mucosal side of the everted small (excluding duodenμM) and large intestine of Sprague-Dawley rats (6 males (m); 6 females (f); 6 pregnant females (pf))	***ZEN-GlcA formation rate:*** • **Jejunum:** (m) 70(10), (f) 50(5), (pf) 80(5) nmol /10cm intestine /h • **P. ileum:** (m) 60(8), (f) 45(5), (pf) 79(12) nmol /10cm intestine /h • **D. ileum:** (m) 52(12), (f) 67(2), (pf) 50(10) nmol /10cm intestine /h • **Colon:** (m) 45(12), (f) 24(6), (pf) 33(7) nmol /10cm intestine /h	(Ieko et al., 2020)
Incubation of hepatic and intestinal rat and human microsomes and individual human UGTs with 50-100 μM ZEN; for up to 1h.	***ZEN- and α-ZEL- GlcA formation rate:*** • **Human liver:** 6(1) nmol/mg protein for both aglycones • **Human intestine:** 5(1) and 4(0) nmol/mg protein for ZEN and α-ZEL respectively • **Rat liver:** 10(1) and 9(1) nmol/mg protein for ZEN and α-ZEL respectively • 14-O-GlcAs were 92; 90 and 87 % of the total GlcAs formed in human liver; human intestinal and rat liver microsomes. Amongst UGT isoforms, UGT1A1, 1A3 and 1A8 showed the highest metabolic activities towards both ZEN and α-ZEL	(Pfeiffer et al., 2010)
	Sulfation	
Exposure to 40 μM ZEN on Caco-2 cells for 3h.	• 5.2 % of ZEN metabolised ZEN sulfate • 16.0 % of *α-ZEL* metabolised to α-ZEL sulfate • 3.1 % of *β-ZEL* metabolised to β-ZEL sulfate	(Pfeiffer et al., 2011)
	Distribution	

IV infusion of 2.25 mg ZEN/h/kg for 6h; until steady state plasma concentration; 4 male Sprague-Swaley rats.	***ZEN*:** • **Tissue-Plasma partition coefficients:** small intestine 26.26, kidney 3.97, liver 2.91, adipose2.28, lung 1.31, heart 0.88, stomach 0.88, brain 0.75, spleen 0.66, testis 0.37, muscle 0.37 • **Blood: Plasma ratio**: 0.75	(Shin et al., 2009)
	Elimination	
Single IV bolus and PO administration of 1-8 mg/kg ZEN in intact and bile-duct cannulated male Sprague-Swaley rats (n=16). TK parameters were determined with non-compartmental analysis.	***ZEN:*** • **$t_{1/2}$, IV bolus:** 0.6(0.3), 1.9(0.9), 1.8(0.7) and 2.8(1.1) h at 1, 2, 4 and 8mg/kg ZEN • **$t_{1/2}$, PO:** 16.8(8.4) (intact), 7.0(5.7) (bile duct-cannulated) h • **CL systemic, IV bolus:** 5.6(1.1), 6.5(2.3), 6.6(3.2) and 5.0(1.4) L/h/kg at 1, 2, 4 and 8mg/kg ZEN • **CL apparent, PO:** (intact)189.9(55.9), (bile duct-cannulated) 414.5(6.3) L/h/kg	(Shin et al., 2009)
Single PO administration of 8 mg/kg *α*-ZEL in female Wistar rats and of 1.23 mg/kg *α*-ZEL in human healthy volunteers (n=6)	***α-ZEL*:** • **Urinary excretion, rat**: 7.5(2.5) % of total dose • **Fecal excretion, rat**: 73.4(11.2) % of total dose • **Fecal excretion; human:** 23.4(10.0) % of total dose • 80 % of the blood and urine concentration in conjugated form	(Migdalof et al., 1983)
Single PO administration of 1 (low) or 100 (high) mg/kg ZEN in female Wistar rats (n=20).	***ZEN:*** • **Urinary excretion, unconjugated**: 16.2(2) / 11.5(1.9) (low/high dose) % of total dose • **Urinary excretion, conjugated:** 2.3(0.7) / 1.9(0.9) (low/high) % of total dose • **Fecal excretion:** 40.3(4.3) / 54.3(3.6) (low/high) % of total dose ***α/ZEL*:** • **Urinary excretion, unconjugated:** 1.4(0.3) / 1.1(0.2) (low/high dose) % of total ZEN dose • **Urinary excretion, conjugated:** 0.4(0.1) / 0.2(0.1) (low/high dose) % of total ZEN dose • **Fecal excretion:** 11.5(1.3) / 9.8(1.1) (low/high dose) % dose	(Fitzpatrick et al., 1988)

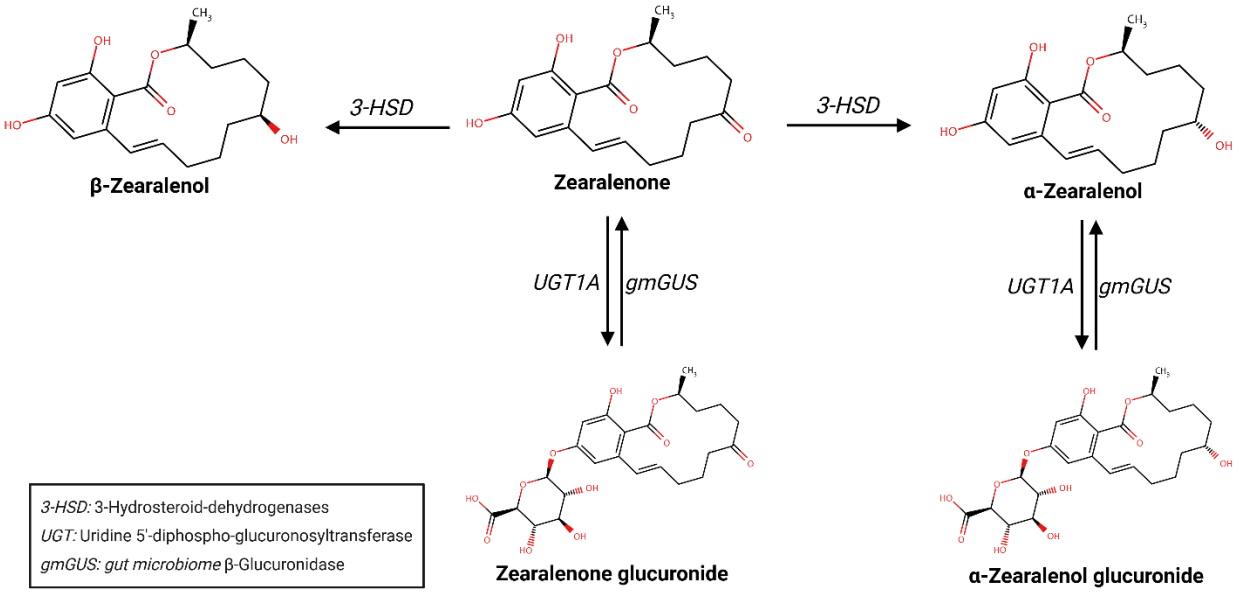

Figure S1: The key pathways of metabolism of Zearalenone in humans and rats, included in this study

Link to github repository: https://doi.org/10.5281/zenodo.20812373

PBK model equations

ZEN and αZEL Aglycones (Agl)

All compartments of the ZEN and αZEL sub-models are the same except the small intestine and liver, where αZEL does not undergo reductive metabolism. As αZEL is only formed in the jejunum, the respective model does not include the duodenum.

Oral dose:

$$\frac{dA_{OD\_Agl}}{dt} = -k_{GER}\, A_{OD\_Agl}$$

Small intestinal lumen:

Duodenum lumen ZEN: $\frac{dA_{DuoL\_ZEN}}{dt} = k_{GER}A_{OD\_ZEN} - k_{duo}A_{DuoL\_ZEN} - CL_{duo\_ZEN}C_{DuoL\_ZEN} - ka_{lymph}A_{DuoL\_ZEN}$

Jejunum lumen aglycones: $\frac{dA_{JejL\_Agl}}{dt} = k_{duo}A_{DuoL\_Agl} - k_{jej}A_{JejL\_Agl} - CL_{jej\_Agl}C_{JejL\_Agl} - ka_{lymph}A_{JejL\_Agl}$

Ileum lumen aglycones: $\frac{dA_{IleL\_Agl}}{dt} = k_{jej}A_{JejL\_Agl} - k_{ile}A_{IleL\_Agl} - CL_{ile\_Agl}C_{IleL\_Agl} - ka_{lymph}A_{IleL\_Agl} + Vmax_{Hydro\_IleL}C_{IleL\_GlcA}/Km_{Hydro} + C_{IleL\_GlcA}$

Small intestine:

Duodenum ZEN: $\frac{dA_{Duo\_ZEN}}{dt} = CL_{duo\_ZEN}C_{DuoL\_ZEN} + Q_{Duo}(C_{B\_ZEN} - CV_{Duo\_ZEN})$

Jejunum ZEN:

$$\frac{dA_{Jej\_ZEN}}{dt} = CL_{jej\_ZEN}C_{Jej\_ZEN} + Q_{Jej}\left(C_{B\_ZEN} - CV_{Jej-ZEN}\right) - Vmax_{SI\_ZENGlcA}C_{Jej\_ZEN}fut_{ZEN}/Km_{SI\_ZENGlcA} + C_{Jej\_ZEN}fut_{ZEN} - Vmax_{SI\_aZEL}C_{Jej\_ZEN}fut_{ZEN}/Km_{SI\_aZEL} + C_{Jej\_ZEN}fut_{ZEN} - Vmax_{SI\_\beta ZEL}C_{Jej\_ZEN}fut_{ZEN}/Km_{SI\_\beta ZEL} + C_{Jej\_ZEN}fut_{ZEN}$$

Jejunum α-ZEL:

$$\frac{dA_{Jej\_aZEL}}{dt} = C_{Jej\_\alpha ZEL} + Q_{Jej}\left(C_{B\_\alpha ZEL} - CV_{Jej\_\alpha ZEL}\right) + Vmax_{SI\_aZEL}C_{Jej\_ZEN}fut_{ZEN}/Km_{SI_{aZEL}} + C_{Jej\_ZEN}fut_{ZEN} - Vmax_{SI\_\alpha ZELGlcA}C_{Jej\_\alpha ZEL}fut_{\alpha ZEL}/Km_{SI\_\alpha ZELGlcA} + C_{Jej\_\alpha ZEL}fut_{\alpha ZEL}$$

Ileum aglycones:

$$\frac{dA_{Ile\_ZEN}}{dt} = CL_{ile\_ZEN}C_{IleL\_ZEN} + Q_{Ile}(C_{B\_ZEN} - CV_{Ile\_ZEN})$$

Liver ZEN:

$$\frac{dA_{L\_ZEN}}{dt} = Q_{Duo}CV_{Duo\_ZEN} + Q_{Jej}CV_{Jej\_ZEN} + Q_{Ile}CV_{Ile\_ZEN} - (Q_{SI} + Q_B)CV_{L\_ZEN} - Vmax_{L\_ZENGlcA}C_{L\_ZEN}fut_{ZEN}/Km_{L\_ZENGlcA} + C_{L\_ZEN}fut_{ZEN} - Vmax_{L\_aZEL}C_{L\_ZEN}fut_{ZEN}/Km_{L\_aZEL} + C_{L\_ZEN}fut_{ZEN} - Vmax_{L\_\beta ZEL}C_{L\_ZEN}fut_{ZEN}/Km_{L\_\beta ZEL} + C_{L\_ZEN}fut_{ZEN}$$

Liver αZEL:

$$\frac{dA_{L\_aZEL}}{dt} = Q_{Duo}CV_{Duo\_aZEL} + Q_{Jej}CV_{Jej\_aZEL} + Q_{Ile}CV_{Ile\_aZEL} - (Q_{SI} + Q_B)CV_{L\_aZEL} - Vmax_{L\_aZELGlcA}C_{L\_aZEL}fut_{aZEL}/Km_{L\_aZELGlcA} + C_{L\_aZEL}fut_{aZEL}$$

Rapidly Perfused Tissue: $\frac{dA_{R\_Agl}}{dt} = Q_R(C_{B\_Agl} - CV_{R\_Agl})$

Slowly Perfused Tissue: $\frac{dA_{S\_ZEN}}{dt} = Q_S(C_{B\_Agl} - CV_{S\_Agl})$

Fat: $\frac{dA_{F\_Agl}}{dt} = Q_F(C_{B\_Agl} - CV_{F\_Agl})$

Blood:

$$\frac{dA_{B\_Agl}}{dt} = ka_{Lymph}(A_{DuoL\_Agl} + A_{JejL\_Agl} + A_{IleL\_Agl}) + CV_{L\_Agl}(Q_{SI} + Q_L) + CV_{F\_Agl}Q_F + CV_{R\_Agl}Q_R + CV_{S\_Agl}Q_S - C_{B\_Agl}(Q_{SI} + Q_L + Q_R + Q_S + Q_F) - GFR\ C_{B\_Agl}\ fup_{Agl}$$

Urine: $\frac{dA_{UR\_Agl}}{dt} = GFR\ C_{B\_Agl}\ fup_{Agl}$

Feces: $\frac{dA_{FE\_Agl}}{dt} = k_{ile}\ A_{IleL\_Agl}$

β-Zearalenol

$$\frac{dA_{\beta ZEL}}{dt} = Vmax_{SI\_\beta ZEL}C_{Jej\_ZEN}ZEN_{fut}/Km_{SI\_\beta ZEL} + C_{Jej\_ZEN}ZEN_{fut} + Vmax_{L\_\beta ZEL}C_{L\_ZEN}ZEN_{fut}/Km_{L\_\beta ZEL} + C_{L\_ZEN}ZEN_{fut}$$

PBK equations for ZEN and αZEL glucuronides (GlcAs)

Small intestinal lumen:

$$\frac{dA_{Duo\_GlcA}}{dt} = CL_{Bile}C_{Bile\_GlcA} - k_{duo}A_{DuoL\_GlcA}$$

$$\frac{dA_{JejL\_GlcA}}{dt} = k_{duo}A_{DuoL\_GlcA} - k_{jej}A_{JejL\_GlcA} + Vmax_{MRP2\_IN}C_{Jej\_IC\_GlcA}fut_{GlcA}/\ Km_{MRP2} + C_{Jej\_IC\_GlcA}\ fut_{GlcA} + Vmax_{BCRP\_IN}C_{Jej\_IC\_GlcA}fut_{GlcA}/\ Km_{BCRP} + C_{Jej\_IC\_GlcA}\ fut_{GlcA}$$

$$\frac{dA_{IleL\_GlcA}}{dt} = k_{jej}A_{JejL\_GlcA} - k_{ile}A_{IleL\_GlcA} - Vmax_{Hydro\_IleL}C_{IleL\_GlcA}/Km_{Hydro} + C_{IleL\_GlcA}$$

Small intestine:

$$\frac{dA_{Jej\_IC\_GlcA}}{dt} = Vmax_{SI\_GlcA}C_{Jej\_Agl}fut_{Agl}/Km_{SI\_GlcA} + C_{Jej\_Agl}fut_{Agl} - Vmax_{MRP2\_IN}C_{Jej\_IC\_GlcA}fut_{GlcA}/\ Km_{MRP2} + C_{Jej\_IC\_GlcA}\ fut_{GlcA} - Vmax_{BCRP\_IN}C_{Jej\_IC\_GlcA}fut_{GlcA}/\ Km_{BCRP} + C_{Jej\_IC\_GlcA}\ fut_{GlcA}$$

$$\frac{dA_{Jej\_EC\_GlcA}}{dt} = Q_{Jej}(C_{B\_GlcA} - CV_{Jej\_GlcA})$$

Liver:

$$\frac{dA_{L\_IC\_GlcA}}{dt} = Vmax_{L\_GlcA} C_{L\_Agl} fut_{Agl} / Km_{L\_GlcA} + C_{L\_Agl} fut_{Agl} - Vmax_{MRP2_{LI}} C_{L\_IC\_GlcA} fut_{GlcA} / Km_{MRP2} + C_{L\_IC\_GlcA} fut_{fut} - Vmax_{MRP3\_LI} C_{L\_IC\_GlcA} fut_{GlcA} / Km_{MRP3} + C_{L\_IC\_GlcA} fut_{GlcA} - Vmax_{BCRP\_LI} C_{L\_IC\_GlcA} fut_{GlcA} / Km_{BCRP} + C_{L\_IC\_GlcA} fut_{GlcA}$$

$$\frac{dA_{L\_EC\_GlcA}}{dt} = Q_{Jej} CV_{Jej\_GlcA} + (Q_L + Q_{Duo} + Q_{Ile)} C_{B\_GlcA} - (Q_L + Q_{SI}) CV_{L\_GlcA} + Vmax_{MRP3\_LI} C_{L\_IC\_GlcA} fut_{GlcA} / Km_{MRP3} + C_{L\_IC\_GlcA} fut_{GlcA}$$

Bile:

$$\frac{dA_{Bile\_GlcA}}{dt} = Vmax_{MRP2\_LI} C_{L\_IC\_GlcA} fut_{GlcA} / Km_{MRP2} + C_{L\_IC\_GlcA} fut_{GlcA} + Vmax_{BCRP\_LI} C_{L\_IC\_GlcA} fut_{GlcA} / Km_{BCRP} + C_{L\_IC\_GlcA} fut_{GlcA} - CL_{Bile} C_{Bile\_GlcA}$$

Rapidly Perfused Tissue: $\frac{dA_{R\_GlcA}}{dt} = Q_R (C_{B\_GlcA} - CV_{R\_GlcA})$

Slowly Perfused Tissue: $\frac{dA_{S\_GlcA}}{dt} = Q_S (C_{B\_GlcA} - CV_{S\_GlcA})$

Fat: $\frac{dA_{F\_GlcA}}{dt} = Q_F (C_{B\_GlcA} - CV_{F\_GlcA})$

Blood:

$$\frac{dA_{B\_GlcA}}{dt} = CV_{L\_GlcA}(Q_{SI} + Q_L) + CV_{F\_GlcA} Q_F + CV_{R\_GlcA} Q_R + CV_{S\_GlcA} Q_S + CV_{K\_GlcA} Q_K - C_{B\_GlcA}(Q_{SI} + Q_L + Q_R + Q_S + Q_F + Q_K) - GFR\ C_{B\_GlcA}\ fup_{GlcA}$$

Kidney:

$$\frac{dA_{K\_GlcA}}{dt} = Q_K \left(C_{B_{GlcA}} - CV_{K_{GlcA}}\right) + GFR\ C_{B\_GlcA}\ fup_{GlcA} - Vmax_{MRP2\_KI} C_{K\_GlcA} fut_{GlcA} / Km_{MRP2} + C_{K\_GlcA}\ fut_{GlcA}$$

Urine: $\frac{dA_{UR\_GlcA}}{dt} = Vmax_{MRP2\_KI} C_{K\_GlcA} fut_{GlcA} / Km_{MRP2} + C_{K\_GlcA}\ fut_{GlcA}$

Feces: $\frac{dA_{FE\_GlcA}}{dt} = k_{ile}\ A_{IleL\_GlcA}$

Table S2: Active transport and metabolism parameters and their respective in vitro-to in vivo scaling values.

Tissue / Enzyme	Parameter	Rat	Human	Reference (R; H)
		Active transport		
Intestine (MRP2)	Vmax	3366e-6	3366e-6	(Li et al., 2019)
	Km	78.9	78.9	
	MGPG	133	133	(Utsey et al., 2020)
	A. in vivo	0.025	3.3	(Couto et al., 2020; Gavins et al., 2023)
	A. in vitro	133.9	133.9	(Li et al., 2019)
	REF	1.8e-4	0.0246	
	f. in-out	0.42	0.42	(Li et al., 2019)
	V. tissue	0.0024	0.2172	
	Scaled Vmax/Km	**3.67e-4**	**162.29**	
Intestine (BCRP)	Vmax	2470e-6	2470e-6	(Li et al., 2019)
	Km	676.4	676.4	
	MGPG	133	133	(Utsey et al., 2020)
	A. in vivo	0.167	0.167	(Couto et al., 2020; Gavins et al., 2023)
	A. in vitro	11.4	11.4	(Li et al., 2019)
	REF	0.015	0.0517	
	f. in-out	0.326	0.326	(Li et al., 2019)
	V. tissue	0.0024	0.2172	
	Scaled Vmax/Km	**0.050**	**42.11**	
Liver (MRP2)	Vmax	3366e-6	3366e-6	(Li et al., 2019)
	Km	78.9	78.9	
	MGPG	210	180	(Utsey et al., 2020)
	A. in vivo	2.08	0.38	(Fallon et al., 2016)
	A. in vitro	133.9	133.9	(Li et al., 2019)
	REF	0.016	0.0028	
	f. in-out	0.42	0.42	(Li et al., 2019)
	V. tissue	0.0052	0.8423	
	Scaled Vmax/Km*	**0.103**	**62.935**	
Liver (MRP3)	Vmax	986.2e-6	986.2e-6	(Li et al., 2019)
	Km	5.7	5.7	
	MGPG	210	180	(Utsey et al., 2020)
	A. in vivo	0.31	0.69	(Fallon et al., 2016)
	A. in vitro	239.4	239.4	(Li et al., 2019)
	REF	0.001	0.0029	
	f. in-out	0.58	0.58	(Li et al., 2019)
	V. tissue	0.0052	0.8423	
	Scaled Vmax/Km	**2.63e-2**	**187.7**	
Liver (BCRP)	Vmax	2470e-6	2470e-6	(Li et al., 2019)
	Km	676.4	676.4	
	MGPG	210	180	(Utsey et al., 2020)
	A. in vivo	0.167	0.13	(Fallon et al., 2016)
	A. in vitro	11.4	11.4	(Li et al., 2019)
	REF	0.015	0.0114	
	f. in-out	0.326	0.326	(Li et al., 2019)
	V. tissue	0.0052	0.8423	
	Scaled Vmax/Km*	**0.11**	**2792.2**	

Kidney (MRP2)	Vmax	3366e-6	3366e-6	(Li et al., 2019)
	Km	78.9	78.9	
	MGPG	180	170	(Utsey et al., 2020)
	A. in vivo	1.4	0.48	(Fallon et al., 2016)
	A. in vitro	133.9	133.9	(Li et al., 2019)
	REF	0.010	0.004	
	f. in-out	0.42	0.42	(Li et al., 2019)
	V. tissue	0.011	0.1488	
	Scaled Vmax/Km*	**1.26**	**132.64**	
		Metabolism		
Intestine (3a-HSD)	Vmax	3.2e-5	3.59e-4	(Malekinejad et al., 2006)
	Km	592	9	
	S9	15.5	35.2	(Doerksen et al., 2021; Peters et al., 2016)
	V.tissue	0.0024	0.2172	
	Scaled Vmax/Km	**1.20e-4**	**18.282**	
Intestine (3b-HSD)	Vmax	7.2e-5	2.09e-4	(Malekinejad et al., 2006)
	Km	21	23	
	S9	15.5	35.2	(Doerksen et al., 2021; Peters et al., 2016)
	V.tissue	0.0024	0.2172	
	Scaled Vmax/Km	**0.008**	**4.174**	
Intestine (UGT1A)-ZEN	Vmax	8.61e-3	4.90e-4	(Mendez-Catala et al., 2021)
	Km	6.20	1.17	
	S9	15.5	35.2	(Doerksen et al., 2021; Peters et al., 2016)
	Alemethicin CF	3	3	(Miners et al., 2021)
	V.tissue	0.0024	0.2172	
	Scaled Vmax/Km	**1.034**	**64.039**	
Intestine (UGT1A)-aZEL	Vmax	6.96e-3	6.96e-3	(Mendez-Catala et al., 2021)
	Km	7.43	7.42	
	S9	15.5	35.2	(Doerksen et al., 2021; Peters et al., 2016)
	Alemethicin CF	3	3	(Miners et al., 2021)
	V.tissue	0.0024	0.2172	
	Scaled Vmax/Km	**0.697**	**143.491**	
Intestine (gmGUS)	Vmax	4.43	5.35	(Ebuzoeme et al., 2021)
	Km	3.08	0.41	
	S9	4	4	(Mendez-Catala et al., 2021)
	V.tissue	0.0041	0.128	(Mendez-Catala et al., 2021)
	Scaled Vmax/Km	**1.41**	**400.86**	
Liver (3a-HSD)	Vmax	3.2e-5	3.59e-4	(Malekinejad et al., 2006)
	Km	592	9	
	S9	46	122	(Mendez-Catala et al., 2021)
	V.tissue	0.0052	0.8423	
	Scaled Vmax/Km	**7.75e-4**	**245.735**	
Liver (3b-HSD)	Vmax	7.2e-5	2.09e-4	(Malekinejad et al., 2006)
	Km	21	23	
	S9	46	122	(Mendez-Catala et al., 2021)
	V.tissue	0.0052	0.8423	
	Scaled Vmax/Km	**0.049**	**56.1073**	
Liver (UGT1A)-ZEN	Vmax	7.03e-3	2.97e-3	(Mendez-Catala et al., 2021)
	Km	6.75	2.043	
	S9	46	122	(Mendez-Catala et al., 2021)
	Alemethicin CF	3	3	(Miners et al., 2021)
	V.tissue	0.0052	0.8423	
	Scaled Vmax/Km	**4.982**	**2665.554**	

Liver (UGT1A)-aZEL	Vmax	6.96e-3	2.98e-3	(Mendez-Catala et al., 2021)
	Km	7.43	2.415	
	S9	46	122	(Mendez-Catala et al., 2021)
	Alemethicin CF	3	3	(Miners et al., 2021)
	V.tissue	0.0052	0.8423	
	Scaled Vmax/Km	**4.483**	**2538.591**	

** Empirically scaled by 10-fold increase*

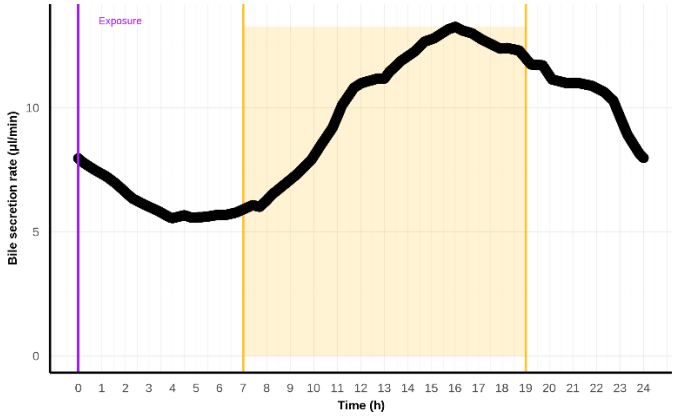

Figure S2: Modelled 24-hour bile secretion rate in rats. Time = 0 corresponds to the start of exposure, which is assumed to be at 8:00 am.

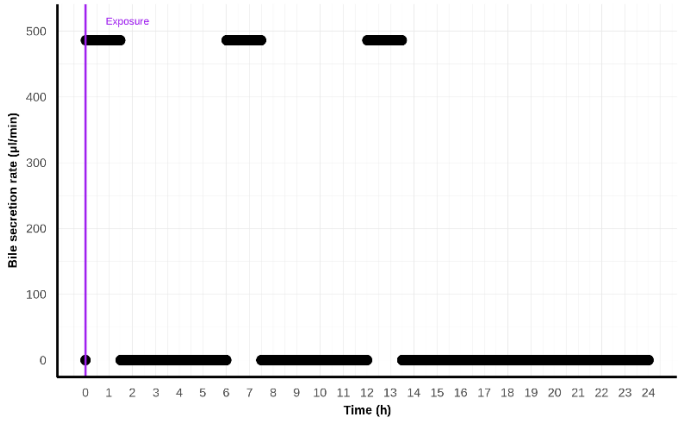

Figure S3: Modelled 24-hour bile secretion rate in humans. Time = 0 corresponds to the start of exposure, which is assumed to be at 8:00 am.

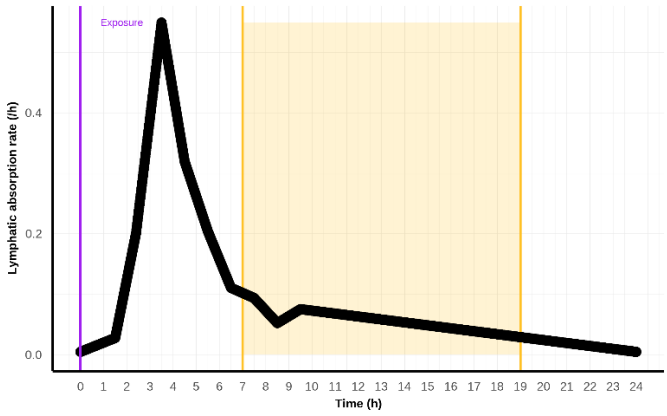

Figure S4: Modelled 24-hour bile secretion rate in humans. Time = 0 corresponds to the start of exposure, which is assumed to be at 8:00 am.

Table S3: In vitro studies and the respective assay, assay medium, derived EC50 and calculated Blood-EC50 used for the QIVIVE.

Assay	Medium	EC50 ZEN (nM)	EC50 αZEL (nM)	Relative Potency Factor	Reference
ERα_CALUX	DMEM/ F12 medium with charcoal stripped serum and non-essential amino-acids	0.490	0.010	51.042	(Ehrlich et al., 2015)
Alkaline phosphatase assay in ishikawa cells	DMEM/F12 supplemented with 5% CD-FBS and 1% P/S	0.359	0.027	13.296	(Grgic et al., 2022)
Alkaline phosphatase assay in ishikawa cells	DMEM/F12 supplemented with 5% CD-FBS stripped of endogenous oestrogen with dextran-coated charcoal	0.058	0.007	8.788	(Le Guevel and Pakdel, 2001)
ERα _CALUX	DMEM/F-12 supplemented with 5% DCC-FCS and 0.5% NEAA	1.580	0.030	52.667	(Mendez-Catala et al., 2020)
MCF-7 bioassay	Phenol red-free DMEM supplemented with 10% dextran-coated charcoal-FBS (10% DCC-FBS)	3.810	0.060	63.500	(Molina-Molina et al., 2014)
MMV-LUC cell line	DMEM and 10% hormone depleted serum	1.600	0.022	72.727	(Frizzell et al., 2011)
MCF-7 bioassay	DMEM containing 10% CD-FCS	1.639	0.050	32.840	(Malekinejad et al., 2006)
MCF-7 bioassay	RPMI medium without phenol red containing 10% DCC-FCS	0.310	0.001	221.429	(Minervini et al., 2005)

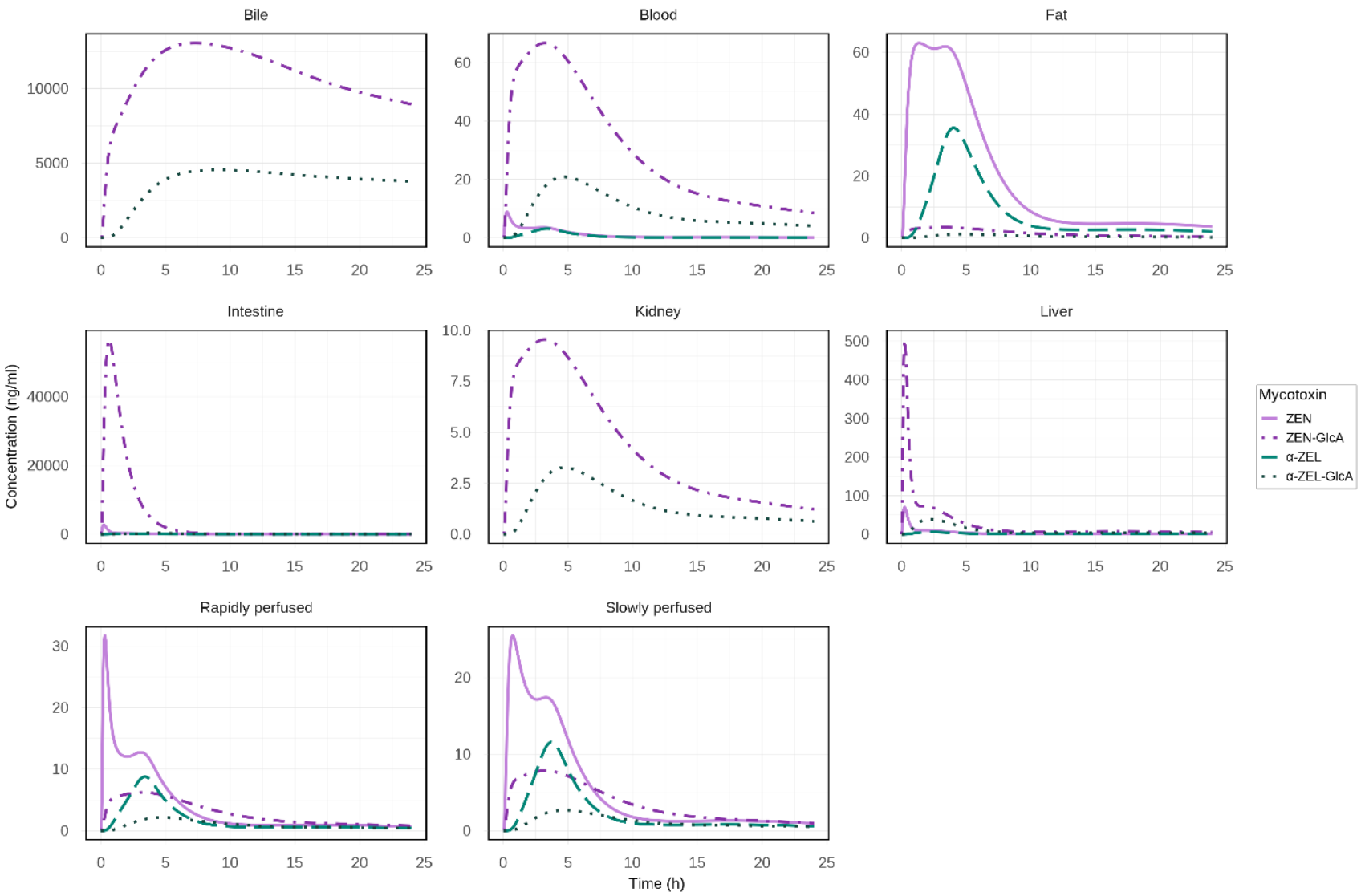

Figure S5: Predicted concentrations of ZEN, α-ZEL, ZEN-GlcA and α-ZEL GlcA in different rat tissues. Green-solid, pink-dashed, dark green-dot-dashed and dark-pink-dotted lines represent ZEN, α-ZEL, ZEN-GlcA and α-ZEL GlcA respectively.

Table S4: Influence of each modelled mechanism on the predicted toxicokinetic parameters of ZEN, ZEN-GlcA, α-ZEL and α-ZEL-GlcA.

	ZEN			**ZEN-GlcA**			**α-ZEL**			**α-ZEL-GlcA**		
	Cmax	**AUC**	**T ½**	**Cmax**	**AUC**	**T ½**	**Cmax**	**AUC**	**T ½**	**Cmax**	**AUC**	**T ½**
mech-PBK	0.185	0.384	11.365	0.067	0.704	12.464	0.034	0.182	11.022	0.015	0.181	14.659
*mech-PBK **w/o** GlcA biliary excretion*	0.185	0.321	1.222	0.067	0.595	3.306	0.033	0.128	1.137	0.014	0.120	2.783
*mech-PBK **w/o** GlcA intestinal excretion*	0.185	0.237	11.236	0.065	0.465	14.051	0.003	0.042	10.880	0.003	0.046	18.146
*mech-PBK **w/o** gmGUS hydrolysis*	0.185	0.188	1.102	0.065	0.382	3.290	0.000	0.000	1.071	0.000	0.000	2.765
*mech-PBK **w/o** lymphatic absorption*	0.185	0.334	11.861	0.067	0.694	12.575	0.014	0.116	11.825	0.014	0.169	15.036

Cmax: maximum concentration in blood
AUC: area under the blood concentration over time curve
T½: half-life
mech-PBK model: the mechanistic-PBK model in rats;
mech-PBK w/o GlcA biliary excretion: the mech-PBK model that does not include the active transport-mediated biliary excretion of GlcAs
mech-PBK w/o GlcA intestinal excretion: the mech-PBK model that does not include the active transport-mediated intestinal excretion of GlcAs
mech-PBK w/o gmGUS hydrolysis: the mech-PBK model that does not include the gmGUS hydrolysis
mech-PBK w/o lymphatic absorption: the mech-PBK model that does not include lymphatic absorption of ZEN and α-ZEL

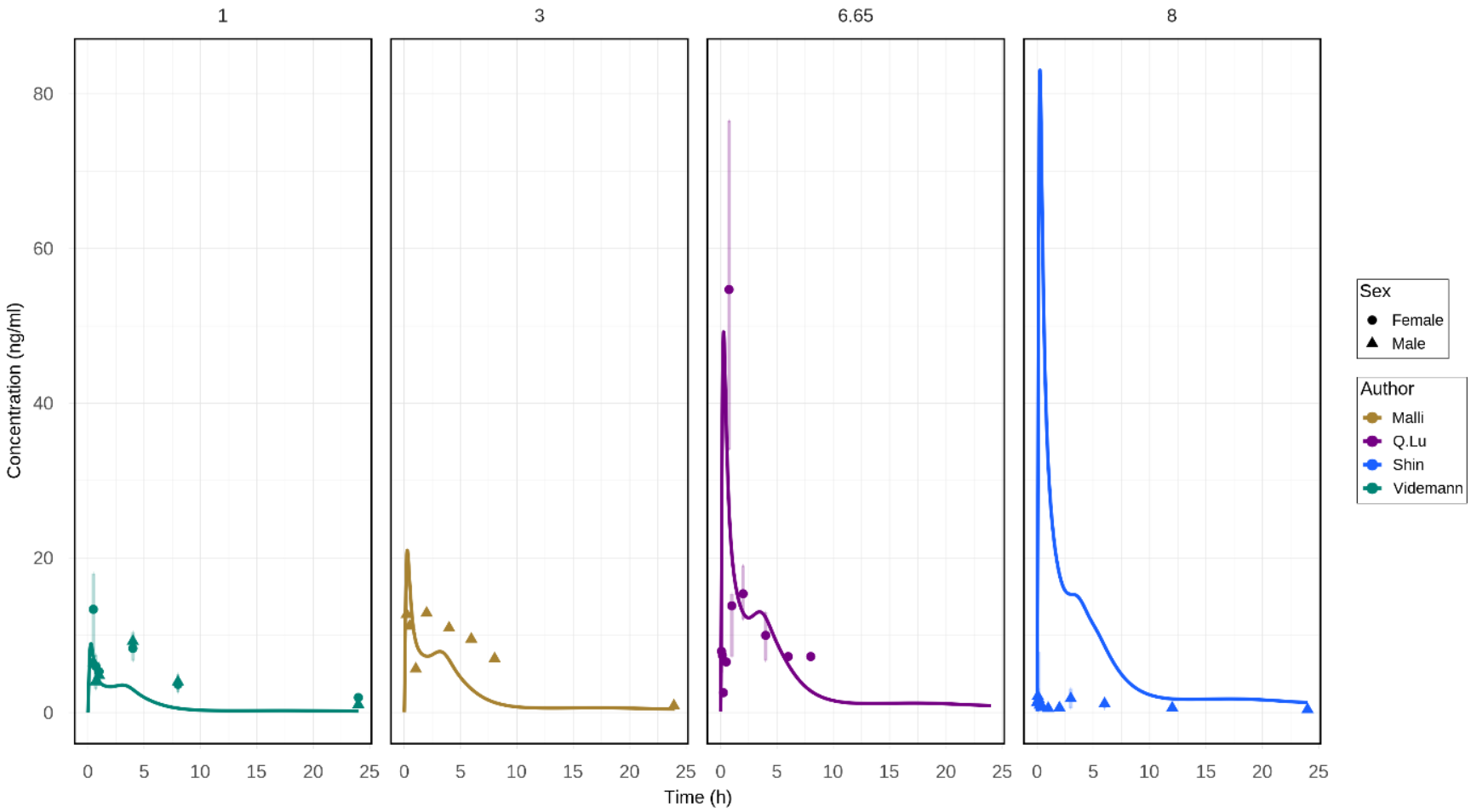

Figure S6: Evaluation of the mechanistic-PBK model against three rat studies. In all studies rats were exposed to ZEN orally. From left to right: (Videmann et al., 2012) in green, dose 1 mg/kg bw; (Mallis et al., 2003) in yellow, dose 3 mg/kg bw; (Lu et al., 2022) in magenta, dose 6.65 mg/kg bw; and (Shin et al., 2009) in blue, dose 8 mg/kg bw. Predicted (solid lines) and observed (points).

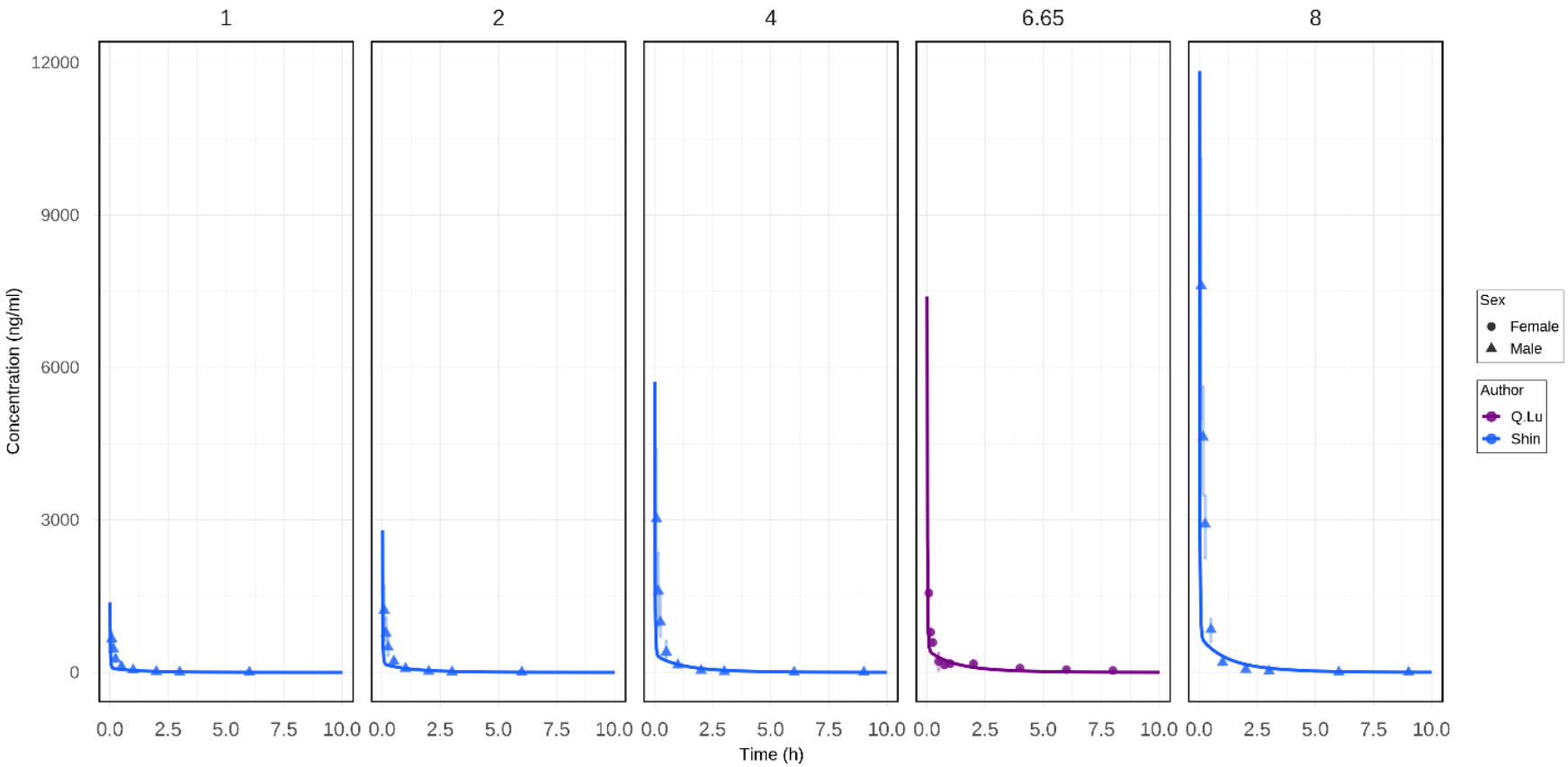

Figure S7: Predicted (solid lines) and observed (points) Zearalenone blood concentration over time curves after IV administration. Data corresponding to the studies of (Lu et al., 2022) and (Shin et al., 2009) are represented in purple, and blue respectively. The panels are separated according to the exposure scheme (1, 2, 4, 6.65 and 8 mg/kg bw/day).

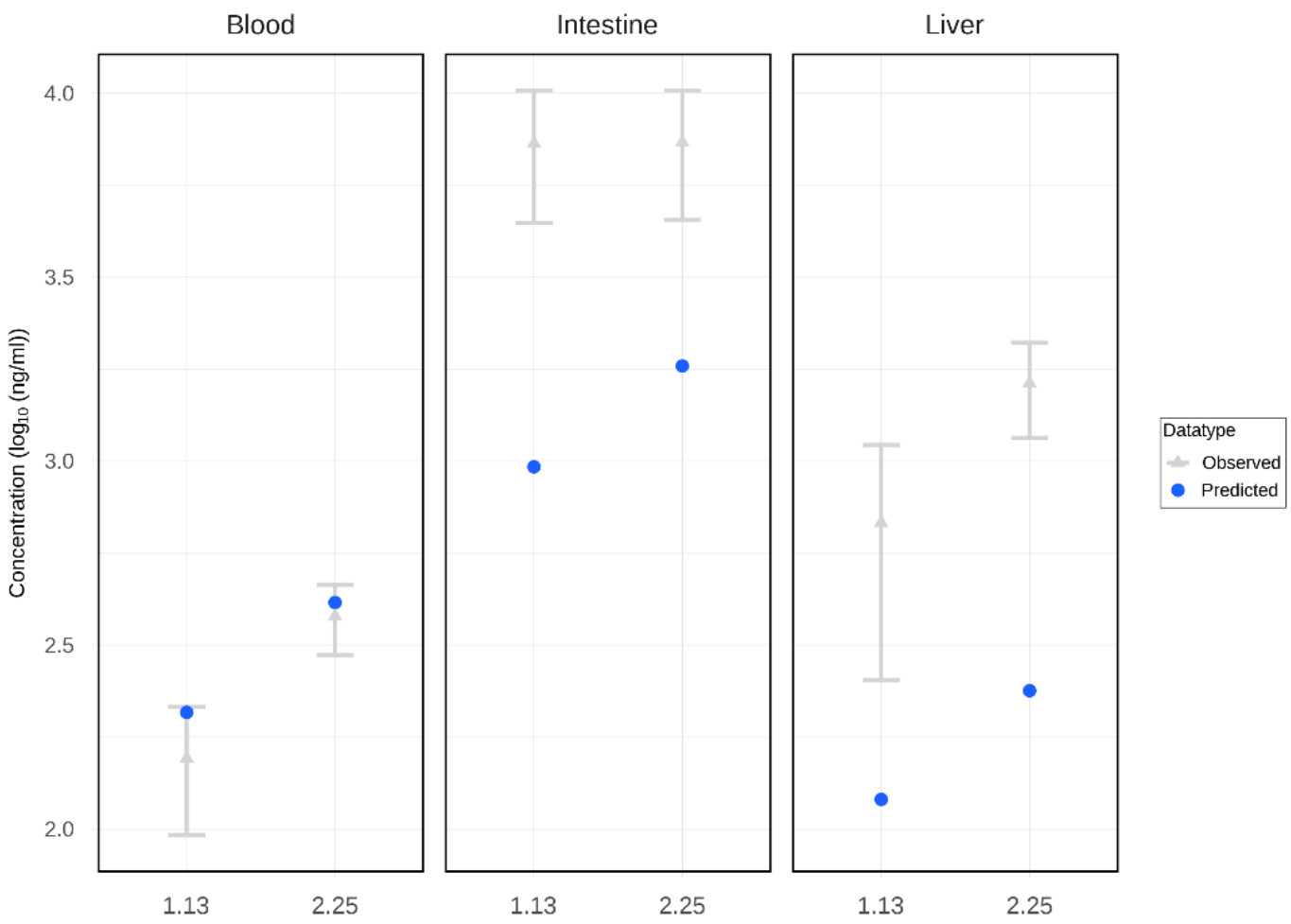

Figure S8: Comparison of the predicted and measured paired blood, liver and intestine concentrations of ZEN, after 6 hours of IV infusion at a low (1.13 mg/h/kg) and high (2.25 mg/h/kg) perfusion rate. The sampling time of 6 hours after continuous perfusion, corresponds to the time needed to reach steady state in the reference study (Shin et al., 2009).Blue circles and grey triangles represent predicted and observed data respectively.

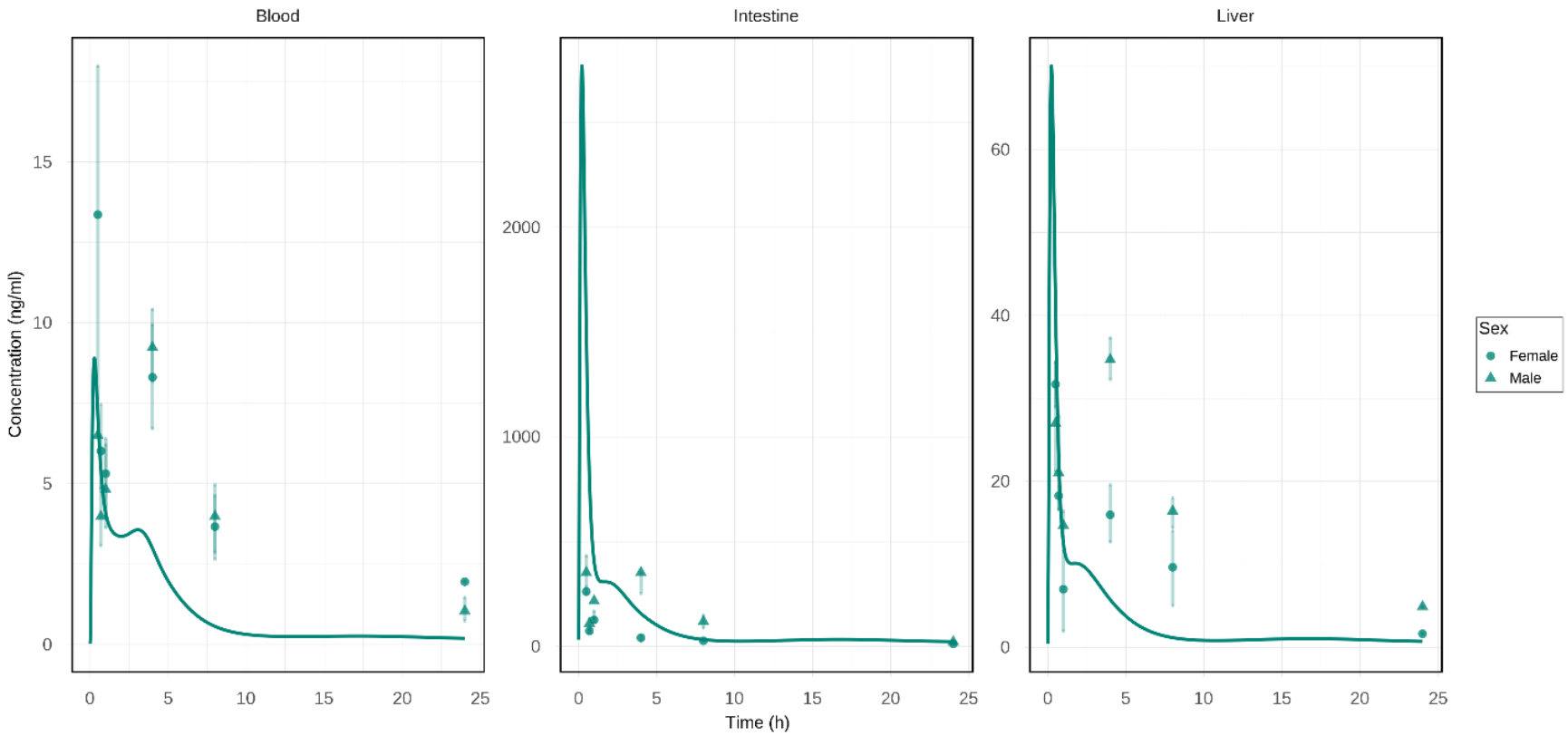

Figure S9: Evaluation of the Mechanistic-PBK model predicted blood, intestinal and liver concentrations of ZEN over time, against those measured in (Videmann et al., 2012). Solid lines and points (circles for females, triangles for males) represent model predictions and measured data respectively.

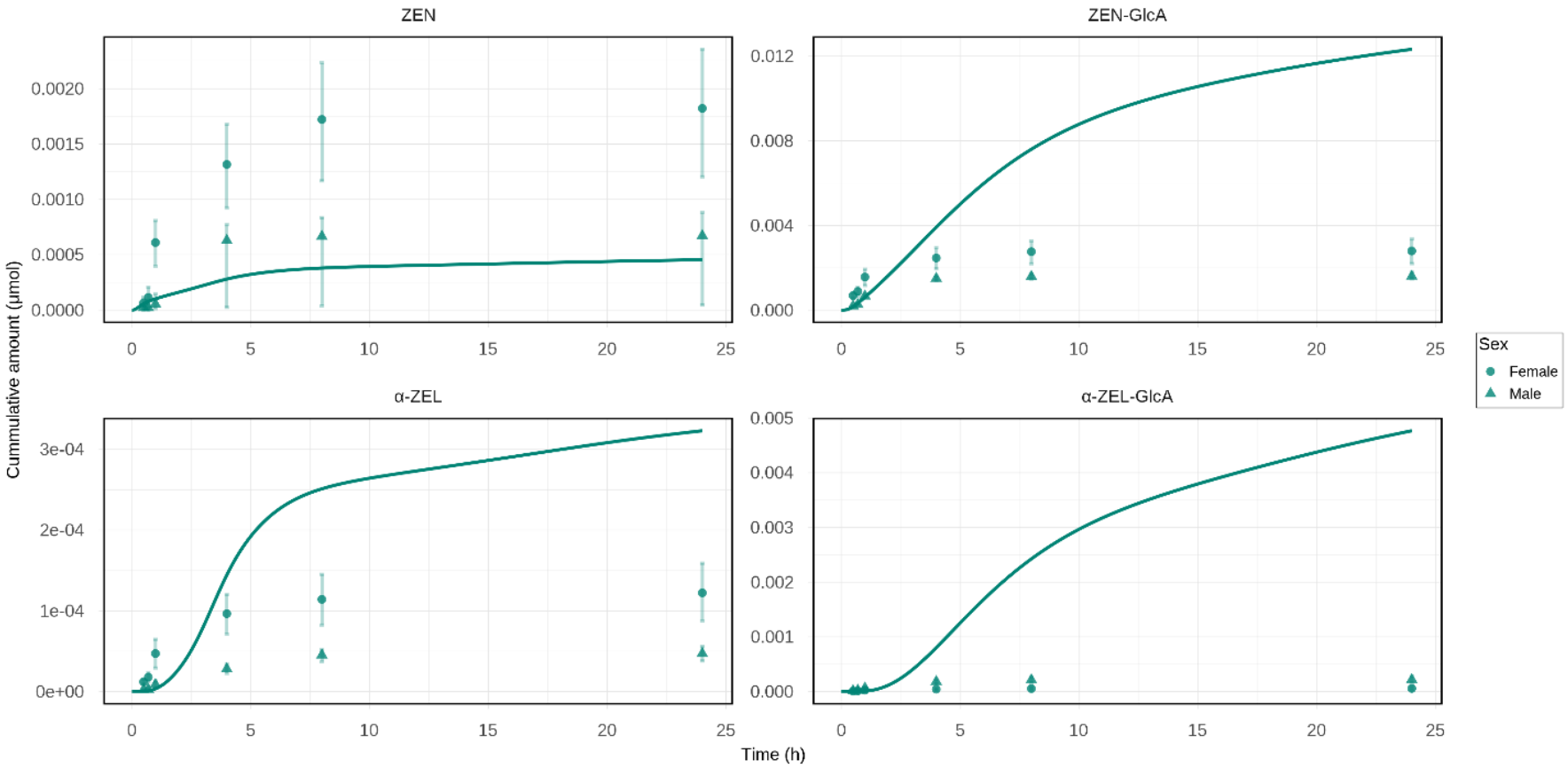

Figure S10: Evaluation of the Mechanistic-PBK model predicted cumulative amounts of ZEN, and its three metabolites in urine over time, against those measured in (Videmann et al., 2012). Solid lines and points (circles for females, triangles for males) represent model predictions and measured data respectively.

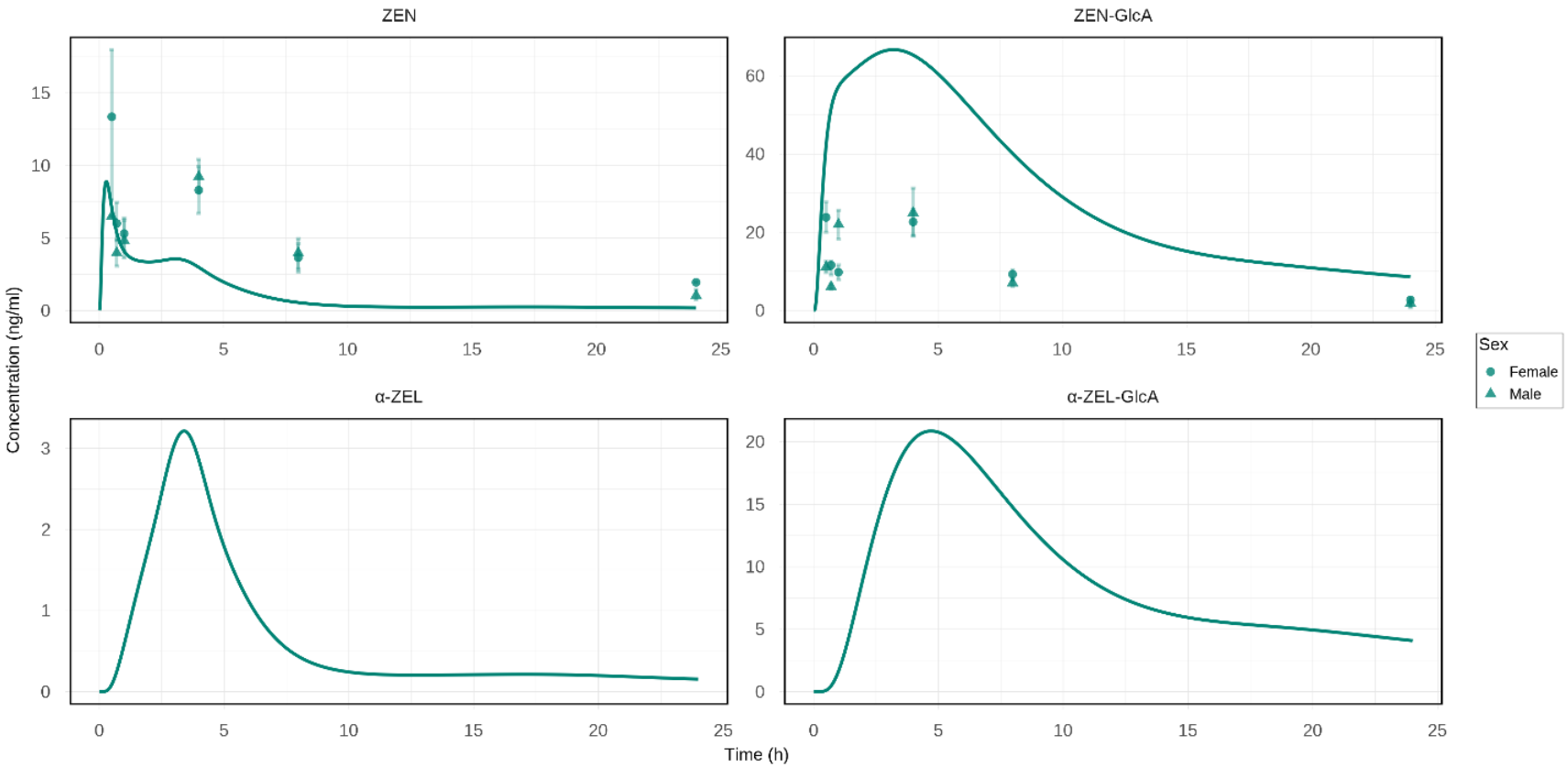

Figure S11: Evaluation of the Mechanistic-PBK model predicted blood concentrations of ZEN, and its three metabolites over time, against those measured in (Videmann et al., 2012). Solid lines and points (circles for females, triangles for males) represent model predictions and measured data respectively. Measured data for αZEL and αZEL-GlcA were below the LOQ and were therefore not available for evaluation.

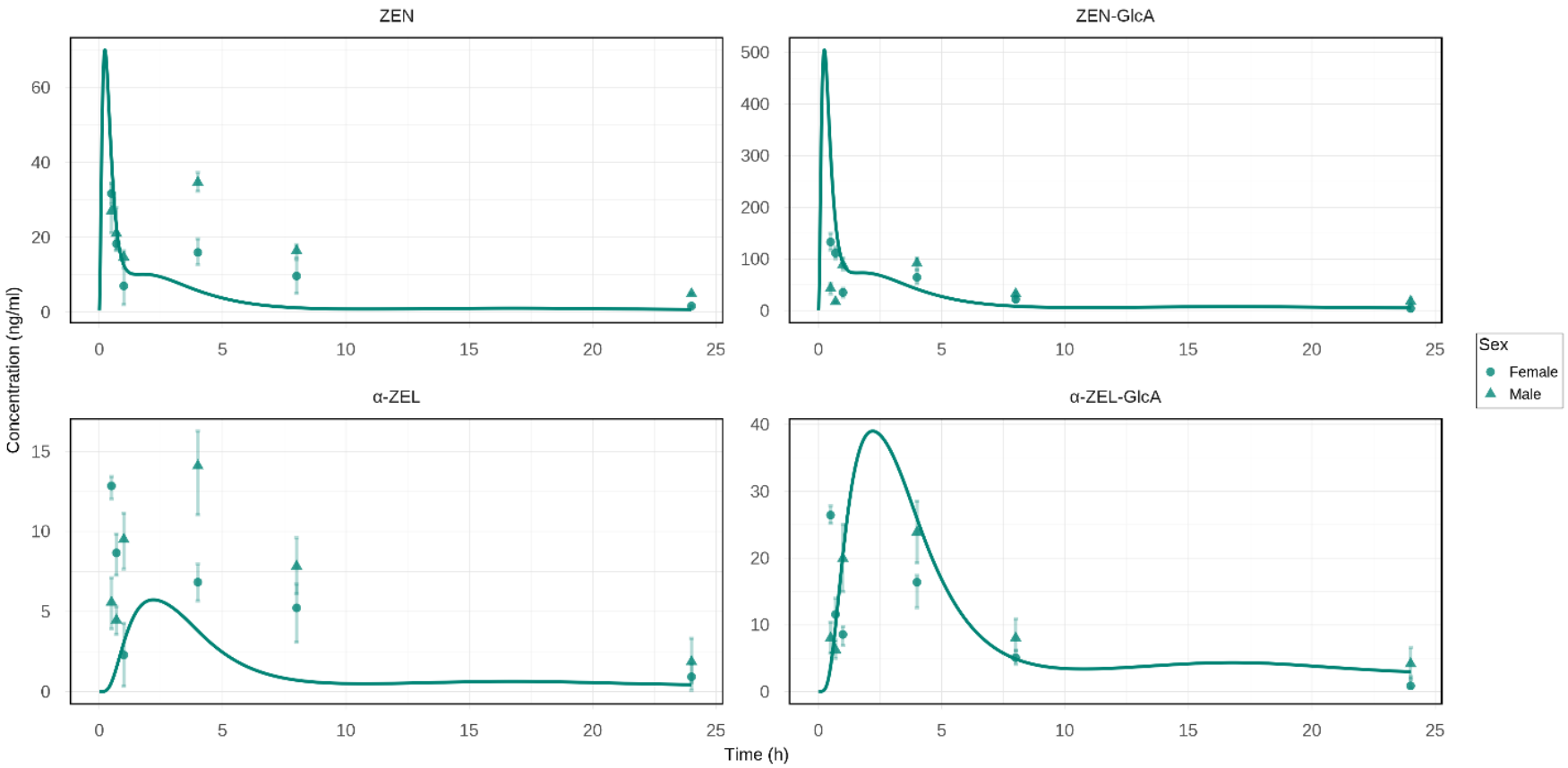

Figure S12: Evaluation of the Mechanistic-PBK model predicted liver concentrations of ZEN, and its three metabolites over time, against those measured in (Videmann et al., 2012). Solid lines and points (circles for females, triangles for males) represent model predictions and measured data respectively.

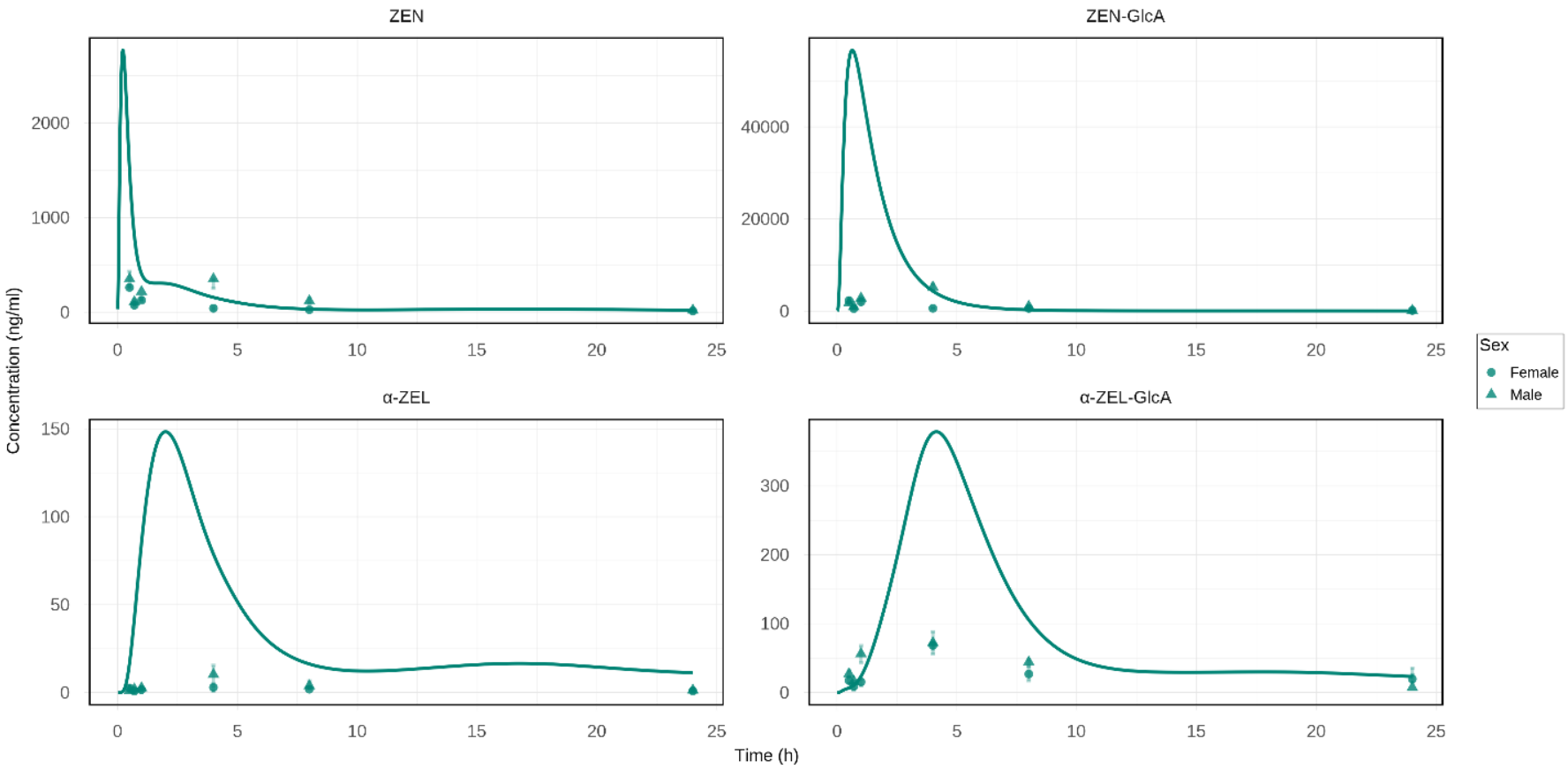

Figure S13: Evaluation of the Mechanistic-PBK model predicted intestinal concentrations of ZEN, and its three metabolites over time, against those measured in (Videmann et al., 2012). Solid lines and points (circles for females, triangles for males) represent model predictions and measured data respectively.

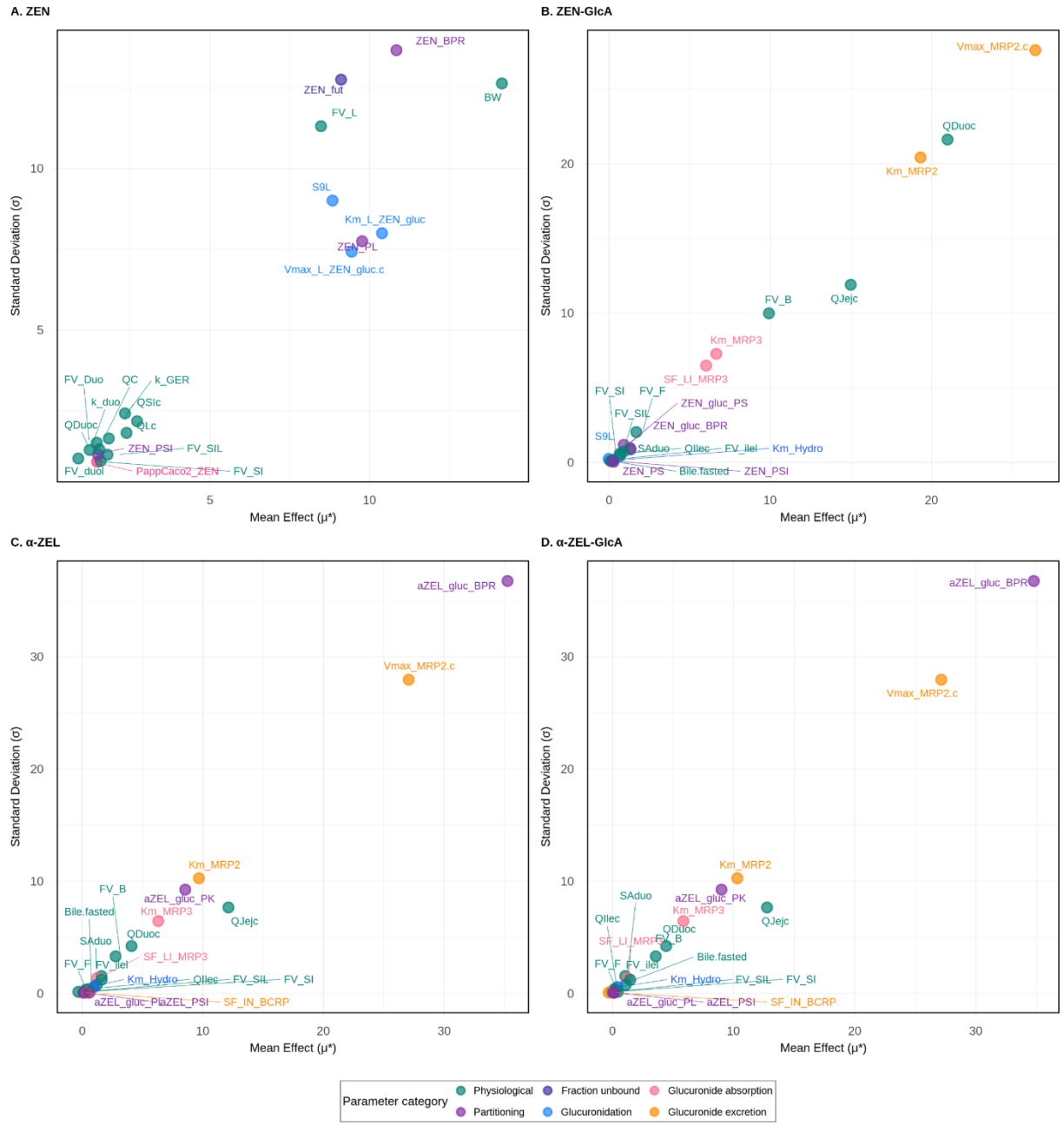

Figure S14: Sensitivity of the rat-PBK model-predicted blood concentration of ZEN (A), ZEN-GlcA (B), α-ZEL (C) and α-ZEL-GlcA (D) according to the Morris Screening test. The graphs show only the 20 most sensitive parameters.

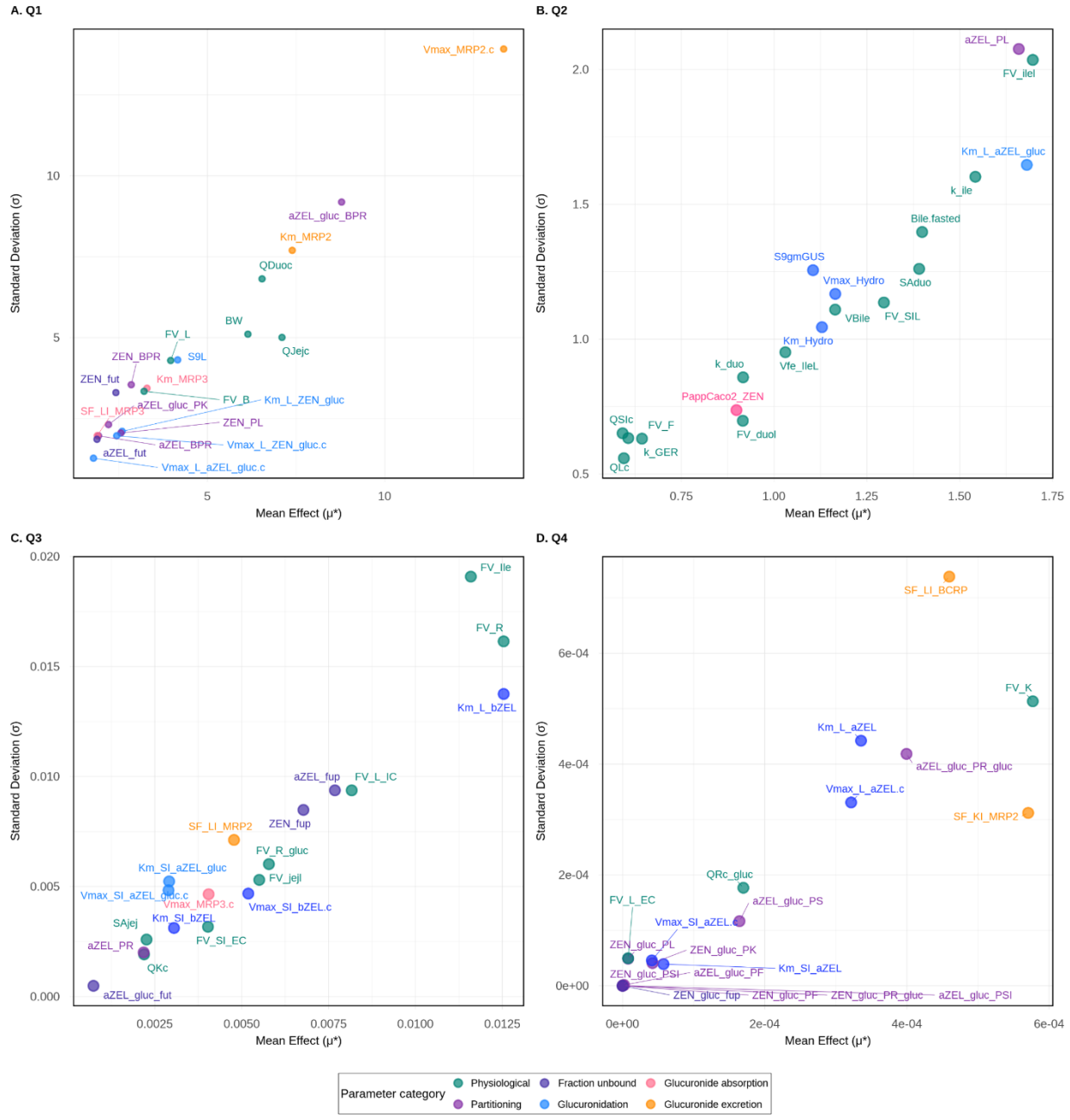

Figure S15: Combined sensitivity of the rat-PBK model-predicted blood concentrations of ZEN, ZEN-GlcA, α-ZEL and α-ZEL-GlcA according to the Morris Screening test, from the most (A.) to the least (D.) sensitive parameters.

Table S5: The most highly ranked parameters towards the predictions of the mech-PBK model in rats, according to the Morris test.

Parameter abbreviation	*Maximum μ**	*Occurrence*
aZEL_gluc_BPR	35.12044646	1
Vmax_MRP2.c	26.73088629	2
QDuoc	20.82457636	3
Km_MRP2	19.67274002	2
QJejc	15.47824976	3
BW	14.32626759	1
ZEN_BPR	11.13329221	1
Km_L_ZEN_gluc	10.04151483	1
ZEN_PL	9.931084223	1
FV_B	9.616027882	2
ZEN_fut	9.486945151	1
Vmax_L_ZEN_gluc.c	9.464797862	1
S9L	8.933429931	3
aZEL_gluc_PK	8.844914369	1
FV_L	8.770934137	1
Km_MRP3	7.006982035	2
SF_LI_MRP3	6.252030603	2
k_GER	2.393179279	1
QLc	2.259402312	1
QSIc	2.252509927	3
FV_SIL	2.109261031	3
FV_F	2.062896934	2
QC	1.672067887	1
FV_ilel	1.491121865	3
PappCaco2_ZEN	1.334865298	3
FV_SI	1.304490067	3
ZEN_PSI	1.268870222	3
k_duo	1.253279443	1
FV_duol	1.211429089	3
FV_Duo	1.210249648	1
SAduo	1.180067452	3
VBile	1.139901465	1
ZEN_gluc_PS	1.139241933	1
Bile.fasted	1.099359542	3
k_ile	1.041715795	1

Maximum μ: the maximum mean effect towards the predicted concentration of ZEN, ZEN-GlcA, α-ZEL and α-ZEL-GlcA*
Occurrence: occurence of the parameter within the 40 most highly ranked parameters across all mycotoxins

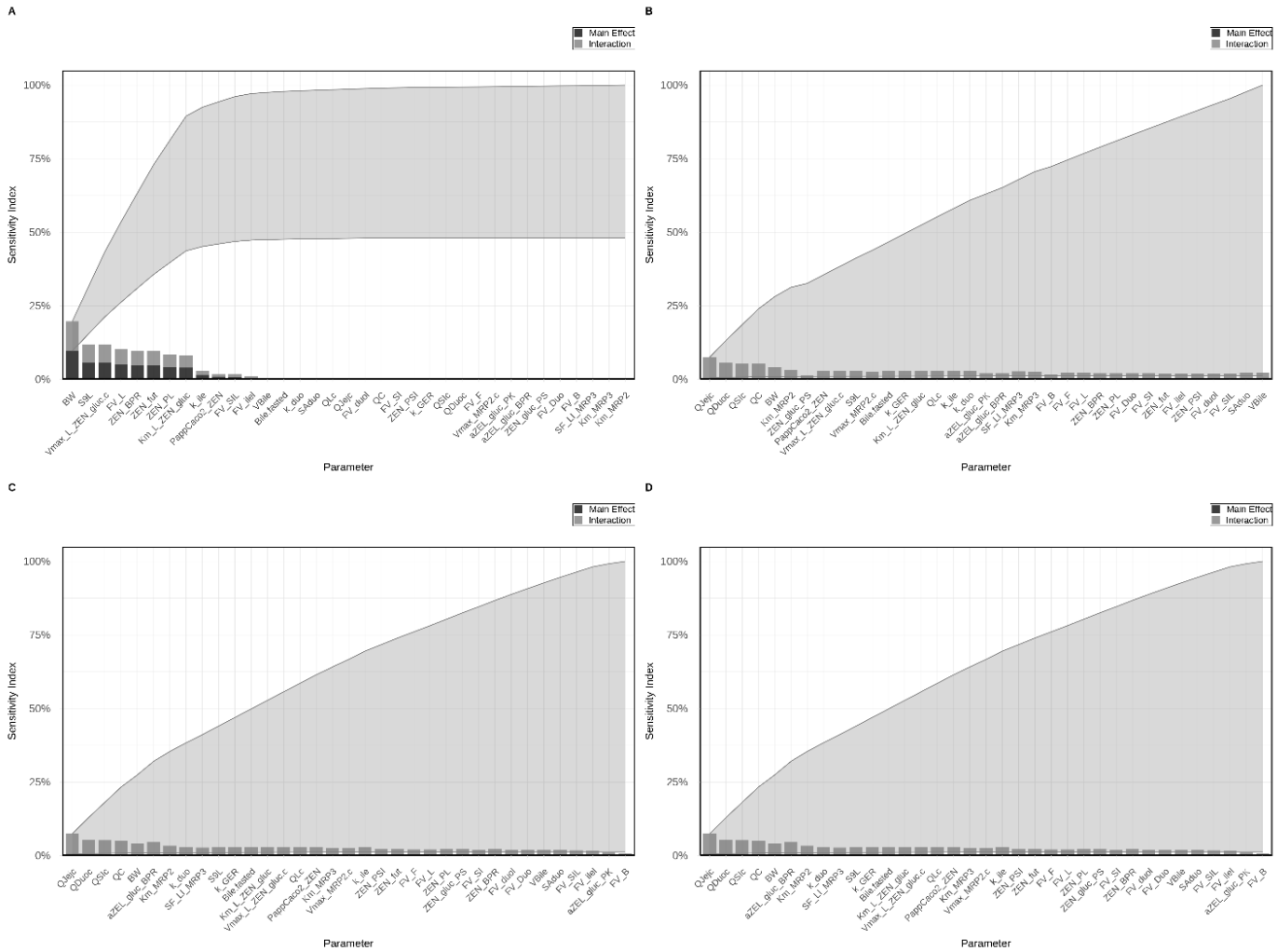

Figure S16: Lowry plots illustrating the results of the eFAST analysis for all model outputs: blood concentration of ZEN (A), ZEN-GlcA (B), α-ZEL (C) and α-ZEL-GlcA (D) of the rat-PBK model. The main effect (dark grey) and interaction (light grey) are stacked on top of each other to reflect the total effect of each parameter. The grey ribbon represents the cumulative effect of all parameters to the model output.

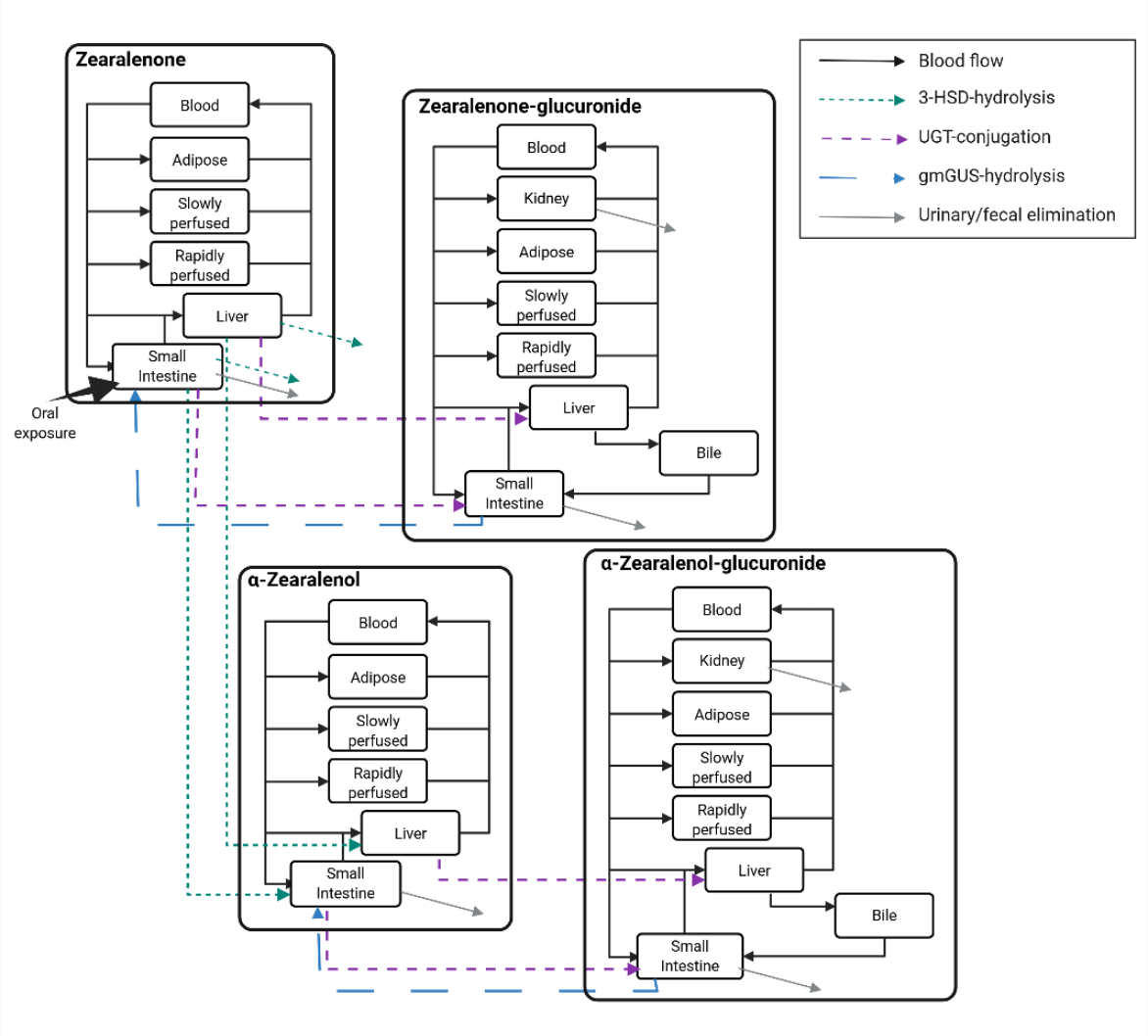

Figure S17. Schematic representation of the human-PBK model for Zearalenone and its metabolites. Solid lines blood and grey lines represent the blood flow and urinary or fecal elimination respectively. Dashed lines represent metabolism; dense-dash green, dash-purple and loose-dash blue lines representing 3-HSD hydrolysis, UGT-conjugation and gmGUS-hydrolysis respectively.

Table S6: Predicted and observed total ZEN (ZEN + ZEN-GlcA[1]) urine levels

	Predicted	**Observed**	**Fold-change**	**Reference**
Total daily cumulative amount in urine (μg)	3 165	32 133	10.14	(Mirocha et al., 1981)
Total daily cumulative amount in urine (μg)	1.49	0.94	1.55	(Warth et al., 2013)
Total concentration in urine (μg/L)[2]	0.032	0.0413 (0.01-0.138)[3]	-	(McKeon et al., 2024)

[1]99.97% ZEN-GlcA; [2] Assuming a total urine volume of 2.42 L; [3] Estimated Daily Intake: 0.0331 µg/kg bw

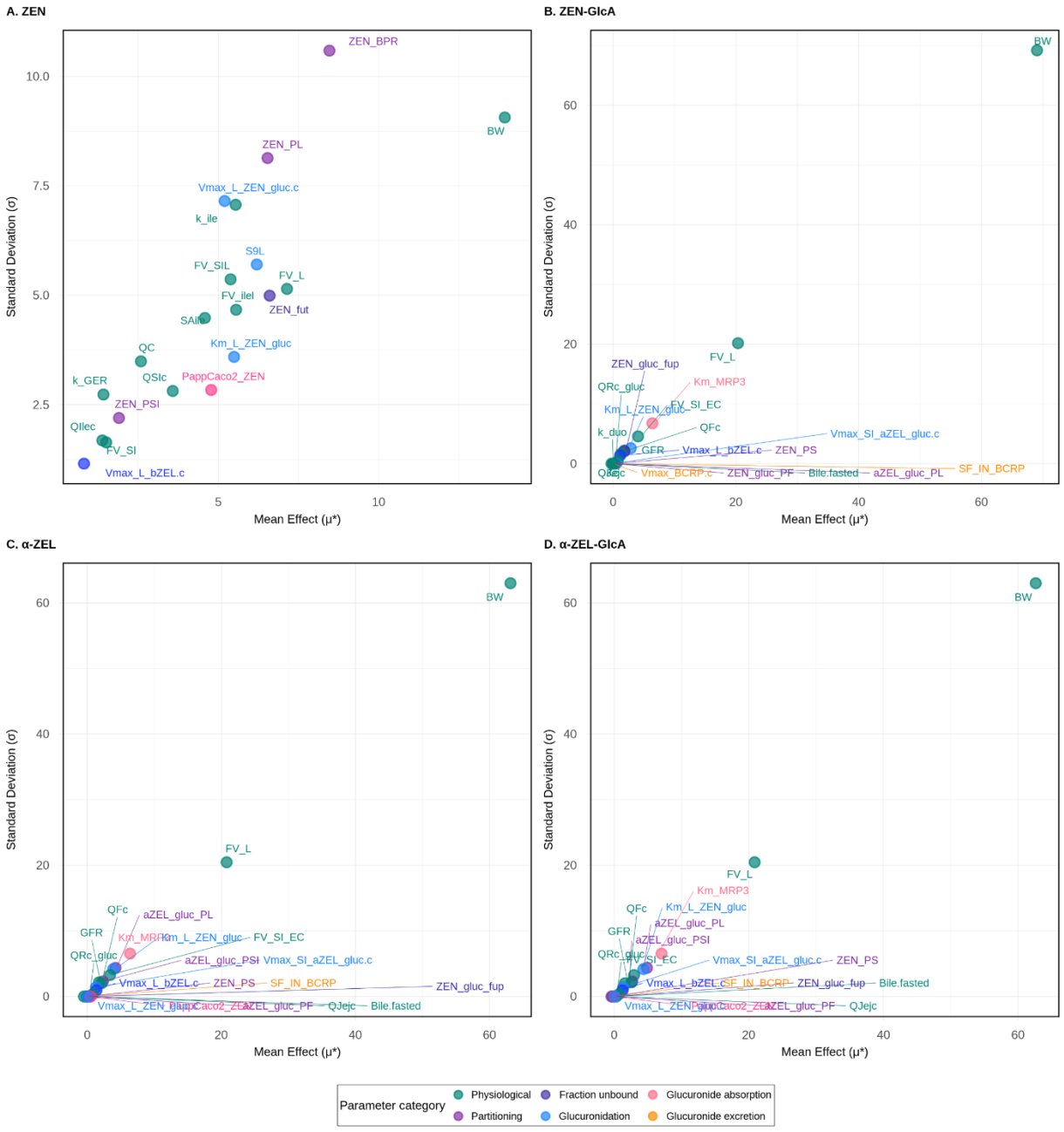

Figure S18: Sensitivity of the rat-PBK model-predicted blood concentration of ZEN (A), ZEN-GlcA (B), α-ZEL (C) and α-ZEL-GlcA (D) according to the Morris Screening test. The graphs show only the 20 most sensitive parameters

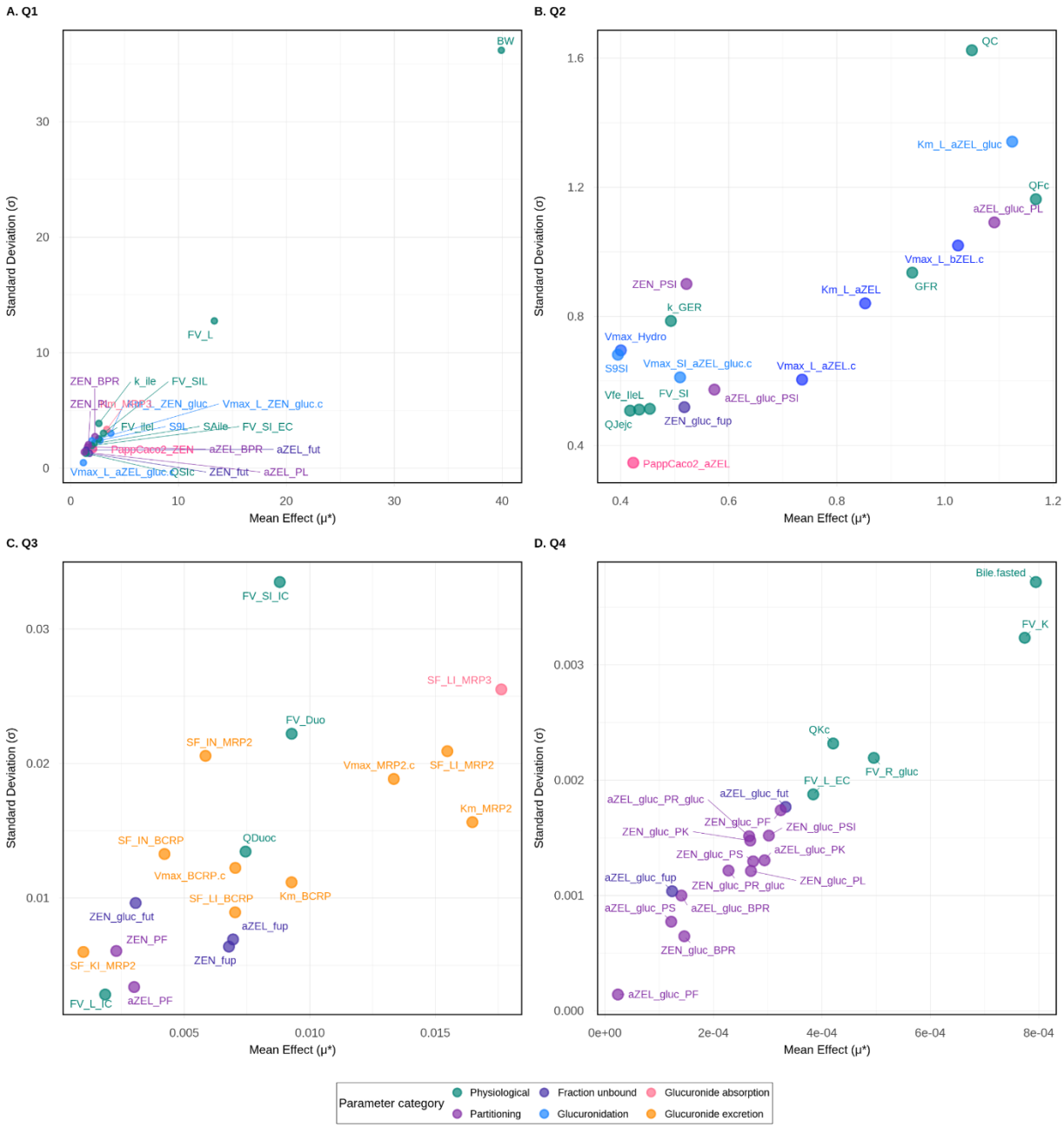

Figure S19: Combined sensitivity of the human-PBK model-predicted blood concentrations of ZEN, ZEN-GlcA, α-ZEL and α-ZEL-GlcA according to the Morris Screening test, from the most (A.) to the least (D.) sensitive parameters.

Table S7: The most highly ranked parameters towards the predictions of the mech-PBK model in humans, according to the Morris test.

Parameter abbreviation	*Maximum μ**	*Occurrence*
BW	69.19731	3
FV_L	20.45681	3
ZEN_BPR	8.751136	1
ZEN_fut	6.76067	3
Km_MRP3	6.75578	2
S9L	6.577332	1
ZEN_PL	6.561391	3
Km_L_ZEN_gluc	5.585515	3
Vmax_L_ZEN_gluc.c	5.489152	3
FV_SIL	5.441808	1
FV_ilel	5.431249	1
k_ile	5.08075	1
SAile	4.908376	2
PappCaco2_ZEN	4.624308	3
FV_SI_EC	4.560292	2
aZEL_gluc_PL	4.362382	2
QSIc	3.455075	2
QC	2.323755	2
aZEL_gluc_PSI	2.293812	1
QFc	2.184042	2
ZEN_gluc_fup	2.067421	2
GFR	2.019644	2
ZEN_PSI	1.68624	1
k_GER	1.449279	1
Vmax_SI_aZEL_gluc.c	1.414741	2
Vmax_L_bZEL.c	1.367118	3
FV_SI	1.197402	1
QIlec	1.148487	1

Maximum μ: the maximum mean effect towards the predicted concentration of ZEN, ZEN-GlcA, α-ZEL and α-ZEL-GlcA*
Occurrence: occurence of the parameter within the 40 most highly ranked parameters across all mycotoxins

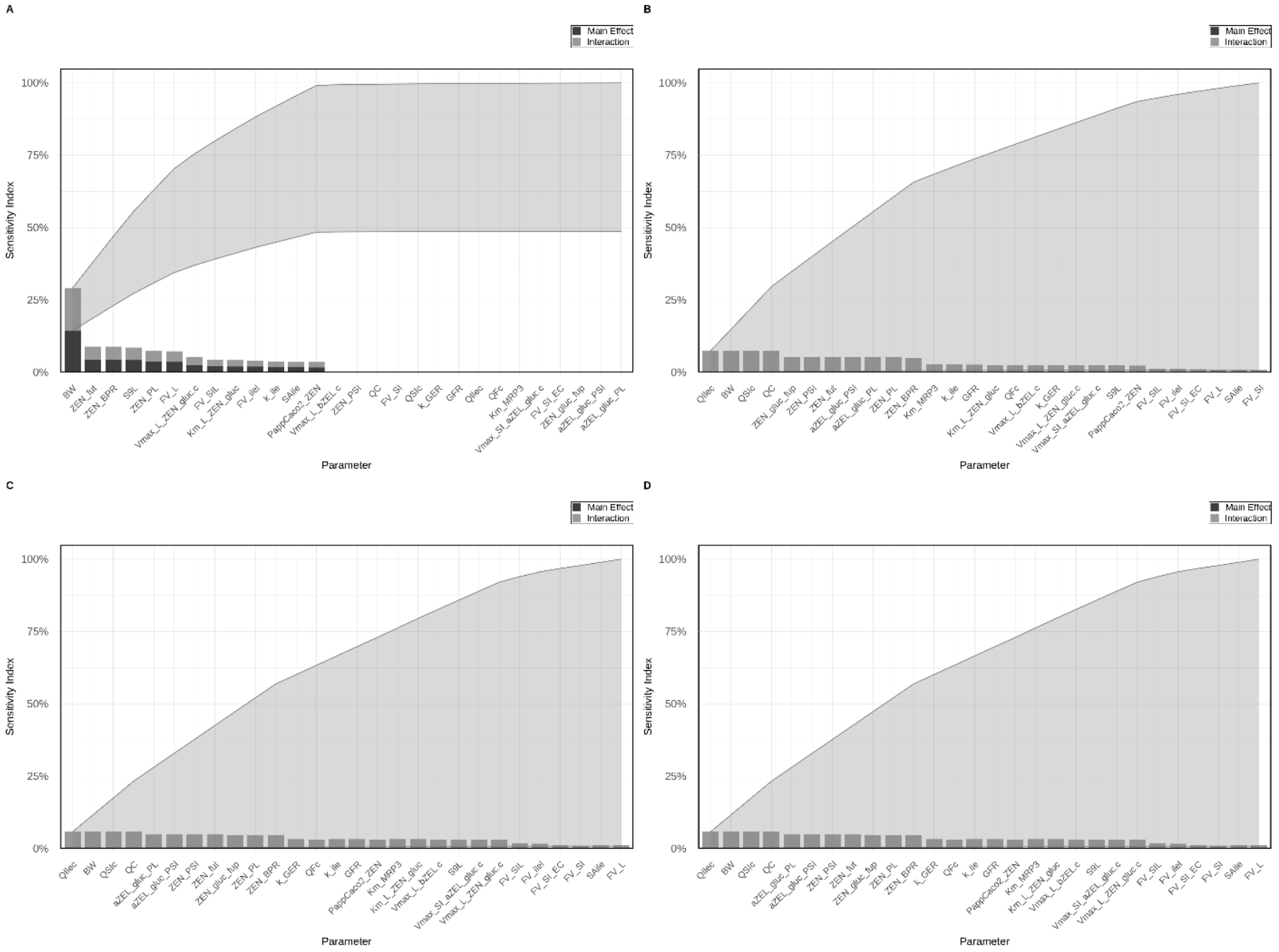

Figure S20: Lowry plots illustrating the results of the eFAST analysis for all model outputs: blood concentration of ZEN (A), ZEN-GlcA (B), α-ZEL (C) and α-ZEL-GlcA (D) of the human-PBK model. The main effect (dark grey) and interaction (light grey) are stacked on top of each other to reflect the total effect of each parameter. The grey ribbon represents the cumulative effect of all parameters to the model output.

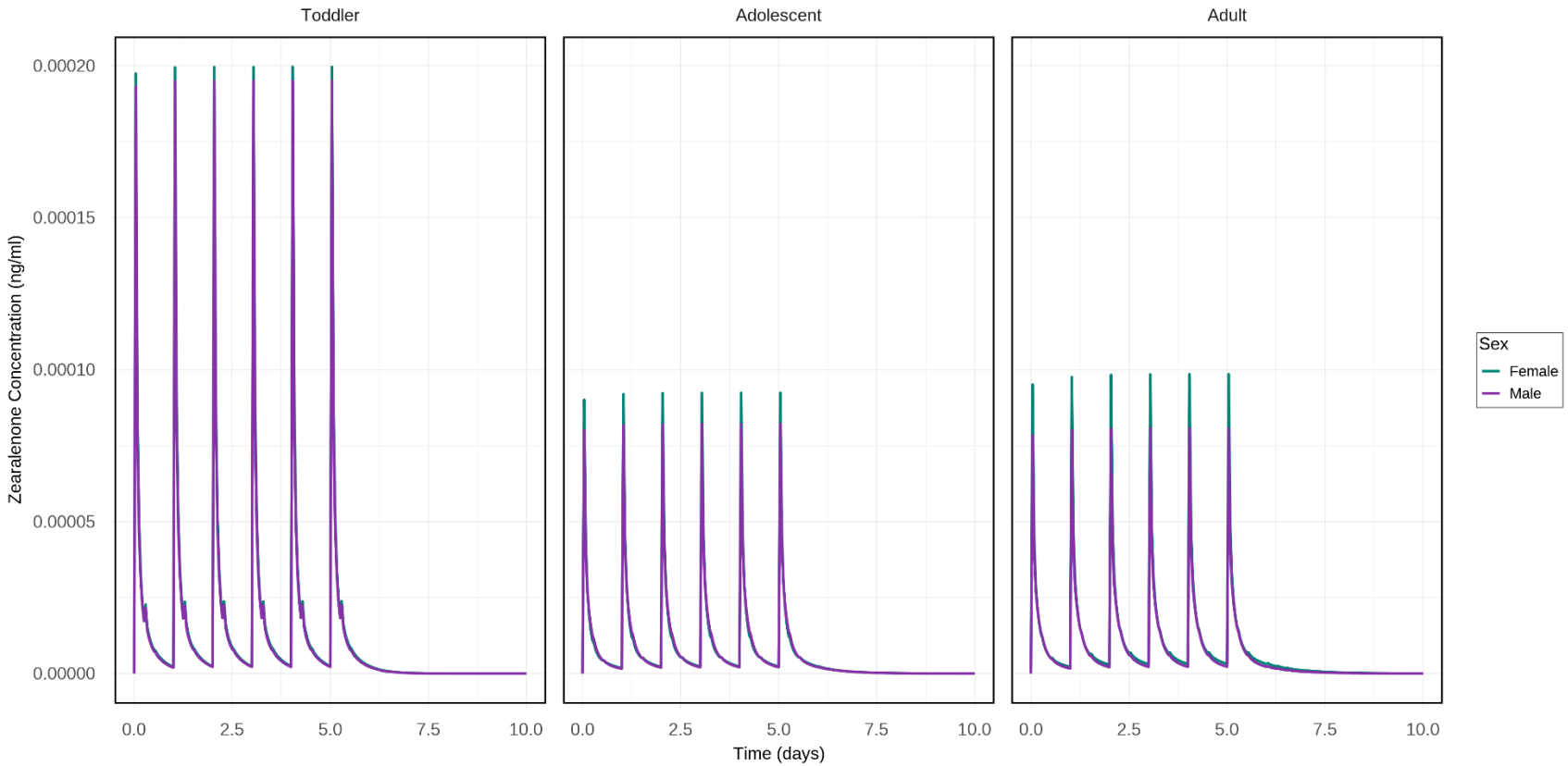

Figure S21: Predicted ZEN blood concentrations in both sexes and different age groups (toddlers, adolescents, adults) after a 6-day-long daily exposure to ZEN of 0.25µg/kg bw/day, corresponding to the TDI. Purple and green lines represent females and males respectively.

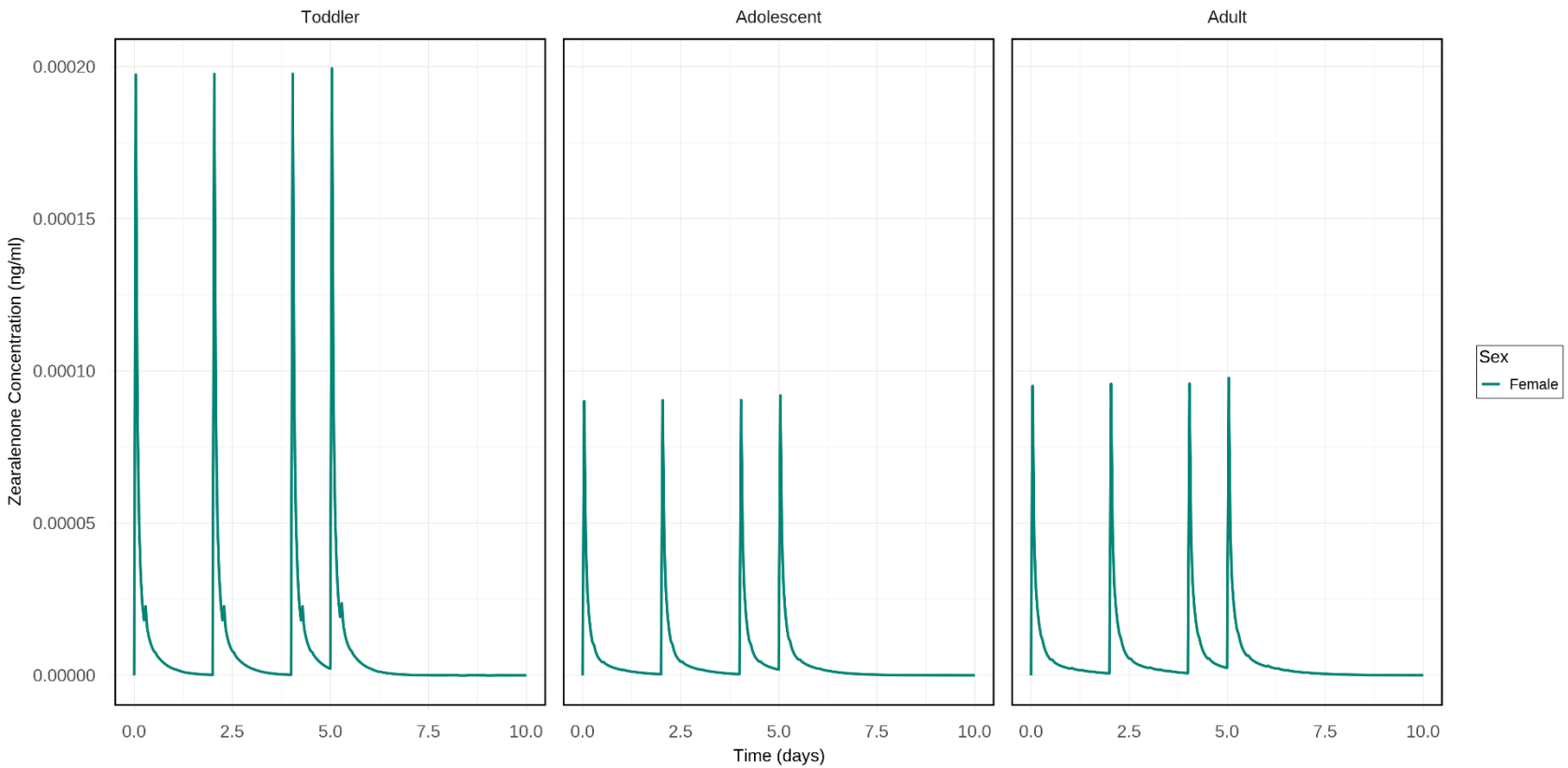

Figure S22: Predicted ZEN blood concentrations in females and different age groups (toddlers, adolescents, adults) after ZEN exposure of 0.25µg/kg bw/day at day 1, 3, 4 and 5, corresponding to the TDI.

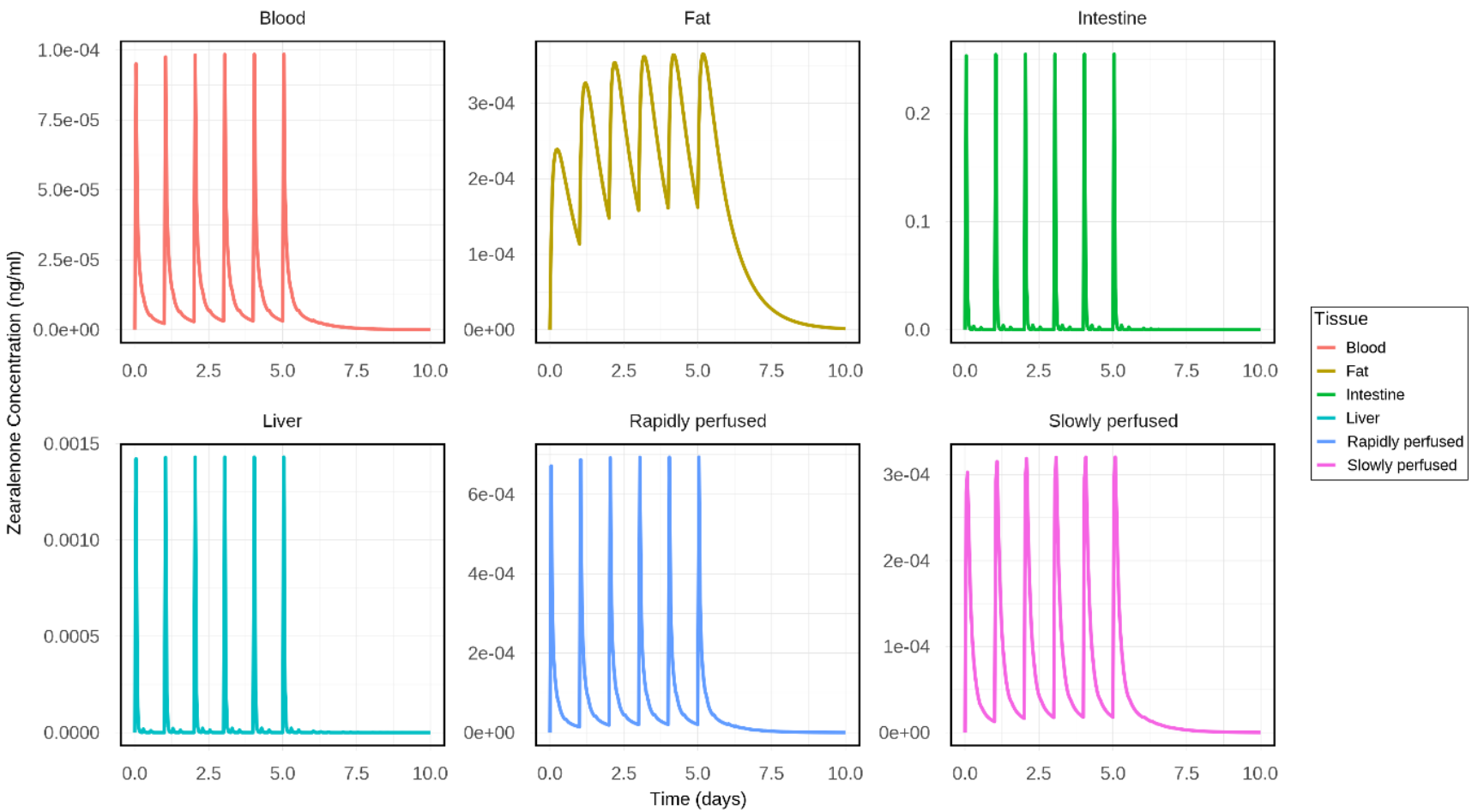

Figure S23: Predicted ZEN tissue concentrations (ng/ml) over time (days), in a 30-year old female. The subject was simulated to have a daily exposure of ZEN of 0.25 ng/kg bw, corresponding to the TDI for 7 days.

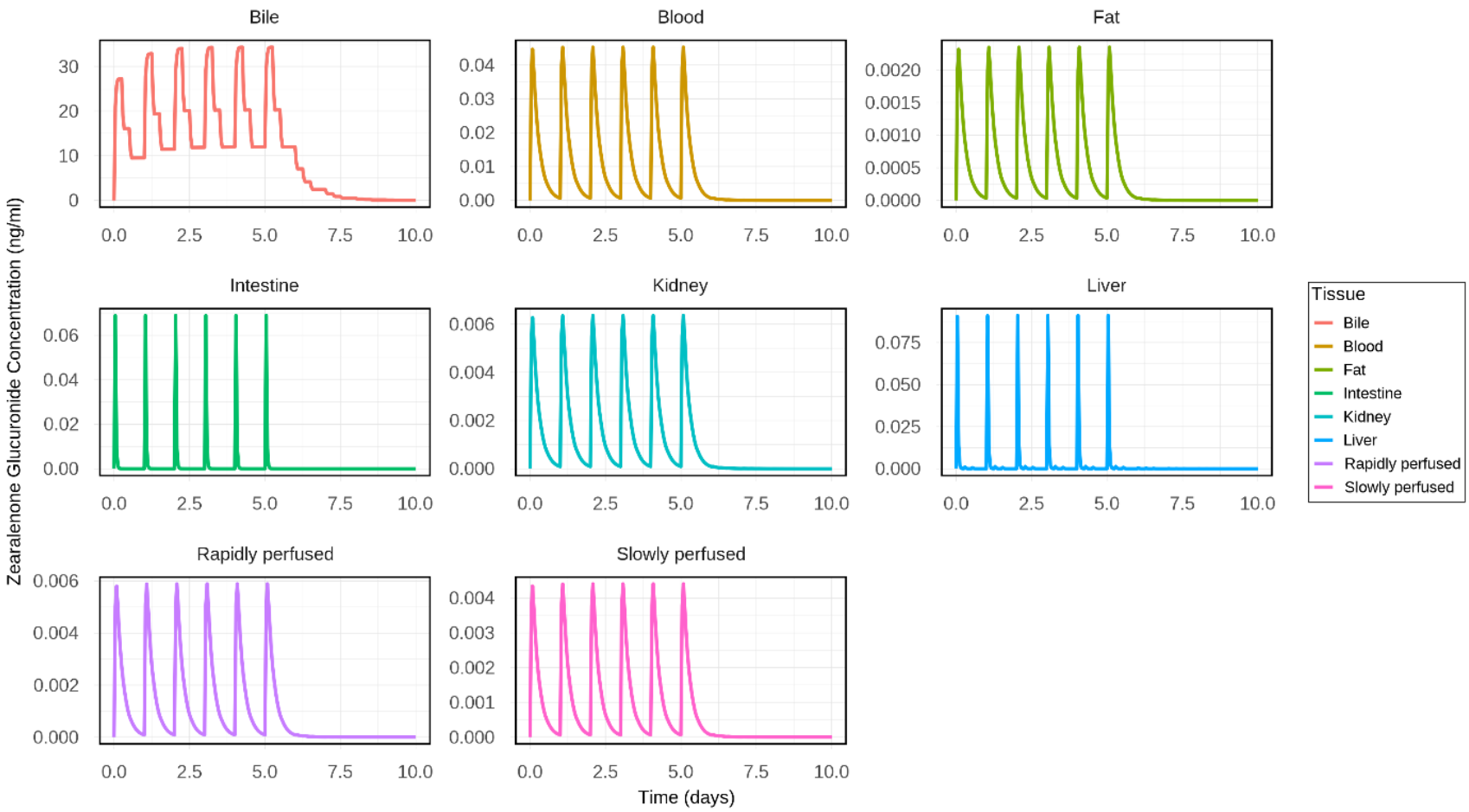

Figure S24: ZEN-GlcA tissue concentrations (ng/ml) over time (days), in a 30-year old female. The subject was simulated to have a daily exposure of ZEN of 0.25 ng/kg bw, corresponding to the TDI for 7 days.

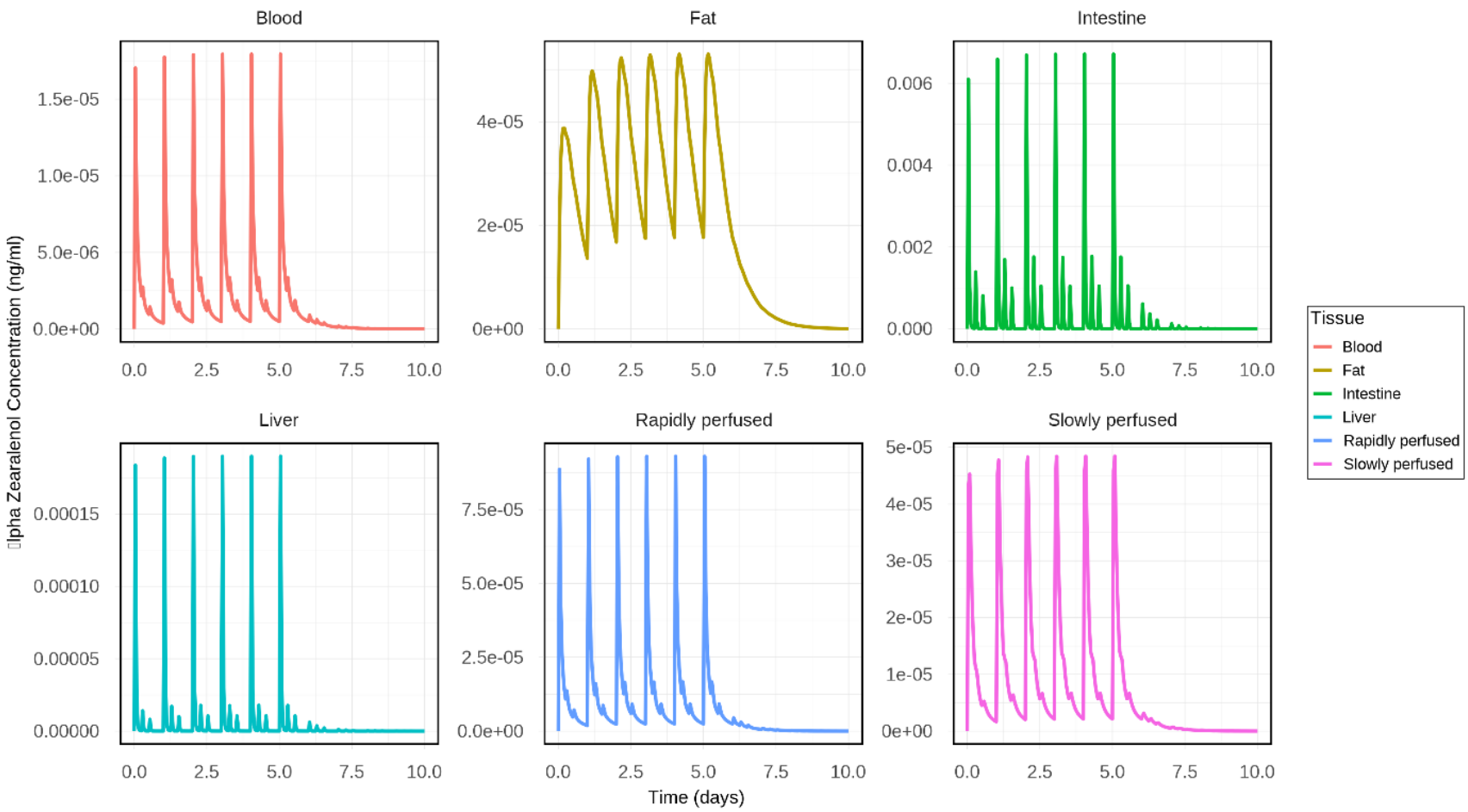

Figure S25: Predicted α-ZEL tissue concentrations (ng/ml) over time (days), in a 30-year old female. The subject was simulated to have a daily exposure of ZEN of 0.25 ng/kg bw, corresponding to the TDI for 7 days.

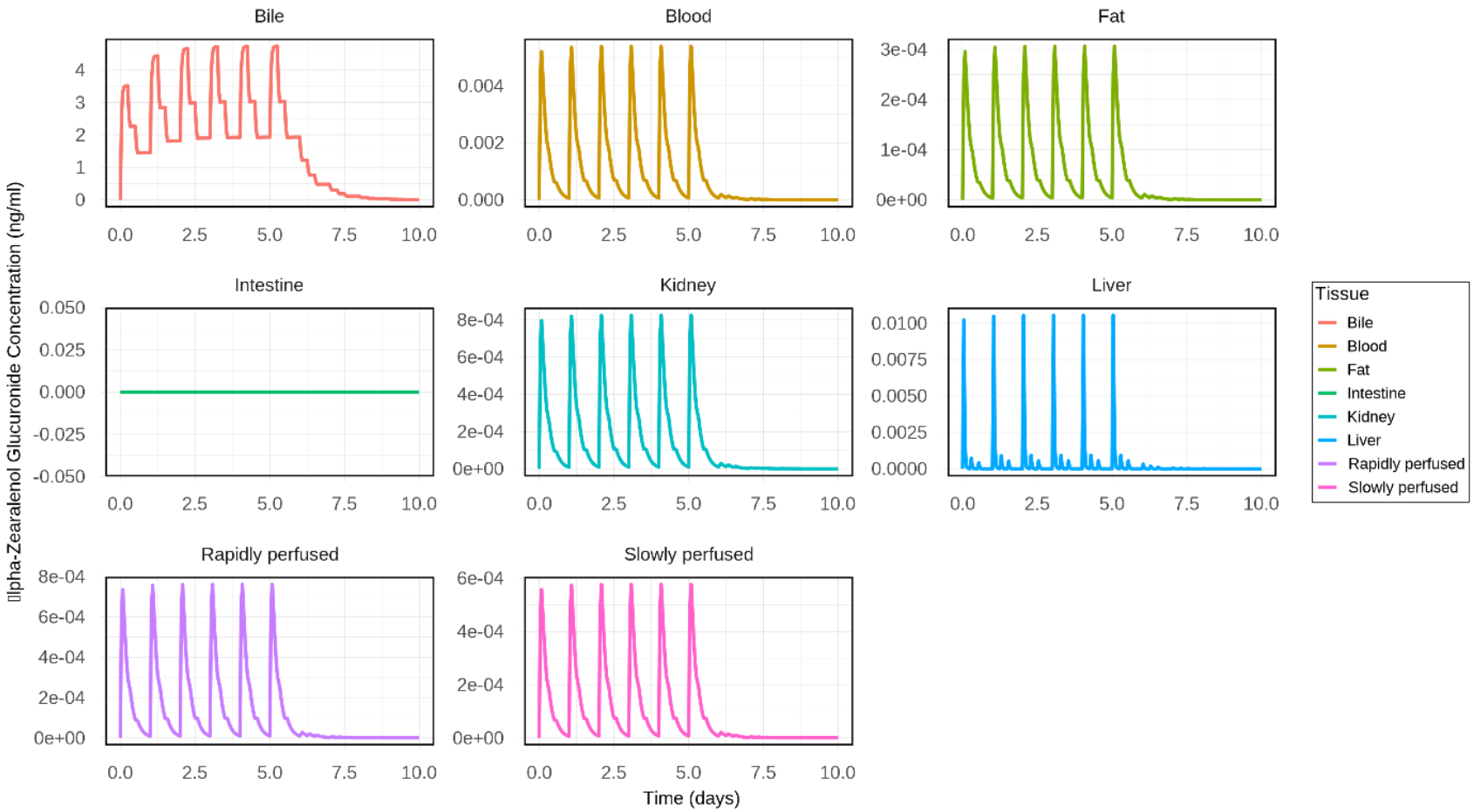

Figure S26: Predicted α-ZEL-GlcA tissue concentrations (ng/ml) over time (days), in a 30-year old female. The subject was simulated to have a daily exposure of ZEN of 0.25 ng/kg bw, corresponding to the TDI for 7 days.

Table S8: QIVIVE results

	Oral Equivalent Dose (µg/kg bw/day)				
Cmax (µM)	ZEN	ZEN + α-ZEL	ZEN + ZEN-GlcA + α-ZEL + α-ZEL-GlcA	Initial assay used to derive the EC50	EC50 reference study
0.00006	24.48	2.19	3.00E-02	Alkaline phosphatase assay (ishikawa cells)	(Le Guevel and Pakdel, 2001)
0.00031	130.84	11.68	0.15	MCF-7 bioassay	(Minervini et al., 2005)
0.00036	151.52	13.53	0.17	Alkaline phosphatase assay (ishikawa cells)	(Grgic et al., 2022)
0.00049	206.81	18.47	0.23	ERα_CALUX	(Ehrlich et al., 2015)
0.00158	666.86	59.56	0.74	ERα _CALUX	(Mendez-Catala et al., 2020)
0.00160	675.31	60.31	0.75	MMV-LUC cell line	(Frizzell et al., 2011)
0.00164	691.77	61.78	0.77	MCF-7 bioassay	(Malekinejad et al., 2006)
0.00381	1608.07	143.61	1.79	MCF-7 bioassay	(Molina-Molina et al., 2014)

References

Couto, N., Al-Majdoub, Z.M., Gibson, S., Davies, P.J., Achour, B., Harwood, M.D., Carlson, G., Barber, J., Rostami-Hodjegan, A., Warhurst, G., 2020. Quantitative Proteomics of Clinically Relevant Drug-Metabolizing Enzymes and Drug Transporters and Their Intercorrelations in the Human Small Intestine. Drug Metab. Dispos. 48, 245–254. https://doi.org/10.1124/dmd.119.089656

Doerksen, M.J., Jones, R.S., Coughtrie, M.W.H., Collier, A.C., 2021. Parameterization of Microsomal and Cytosolic Scaling Factors: Methodological and Biological Considerations for Scalar Derivation and Validation. Eur. J. Drug Metab. Pharmacokinet. 46, 173–183. https://doi.org/10.1007/s13318-020-00666-w

Ebuzoeme, C., Etim, I., Ikimi, A., Song, J., Du, T., Hu, M., Liang, D., Gao, S., 2021. Glucuronides Hydrolysis by Intestinal Microbial β-Glucuronidases (GUS) Is Affected by Sampling, Enzyme Preparation, Buffer pH, and Species. Pharmaceutics 13, 1043. https://doi.org/10.3390/pharmaceutics13071043

Ehrlich, V.A., Dellafiora, L., Mollergues, J., Dall'Asta, C., Serrant, P., Marin-Kuan, M., Piparo, E.L., Schilter, B., Cozzini, P., 2015. Hazard assessment through hybrid in vitro/in silico approach: the case of zearalenone. ALTEX - Altern. Anim. Exp. 32, 275–286. https://doi.org/10.14573/altex.1412232

Fallon, J.K., Smith, P.C., Xia, C.Q., Kim, M.-S., 2016. Quantification of Four Efflux Drug Transporters in Liver and Kidney Across Species Using Targeted Quantitative Proteomics by Isotope Dilution NanoLC-MS/MS. Pharm. Res. 33, 2280–2288. https://doi.org/10.1007/s11095-016-1966-5

Fitzpatrick, D.W., Arbuckle, L.D., Hassen, A.M., 1988. Zearalenone metabolism and excretion in the rat: Effect of different doses. J. Environ. Sci. Health Part B 23, 343–354. https://doi.org/10.1080/03601238809372610

Frizzell, C., Ndossi, D., Verhaegen, S., Dahl, E., Eriksen, G., Sørlie, M., Ropstad, E., Muller, M., Elliott, C.T., Connolly, L., 2011. Endocrine disrupting effects of zearalenone, alpha- and beta-zearalenol at the level of nuclear receptor binding and steroidogenesis. Toxicol. Lett. 206, 210–217. https://doi.org/10.1016/j.toxlet.2011.07.015

Gavins, F.K.H., Dou, L., Qin, Y., Madla, C.M., Murdan, S., Basit, A.W., Mai, Y., Orlu, M., 2023. Prandial state and biological sex modulate clinically relevant efflux transporters to different extents in Wistar and Sprague Dawley rats. Biomed. Pharmacother. 160, 114329. https://doi.org/10.1016/j.biopha.2023.114329

Grgic, D., Betschler, A., Früholz, R., Novak, B., Varga, E., Marko, D., 2022. Estrogenic in vitro evaluation of zearalenone and its phase I and II metabolites in combination with soy isoflavones. Arch. Toxicol. 96, 3385–3402. https://doi.org/10.1007/s00204-022-03358-3

Ieko, T., Inoue, S., Inomata, Y., Inoue, H., Fujiki, J., Iwano, H., 2020. Glucuronidation as a metabolic barrier against zearalenone in rat everted intestine. J Vet Med Sci 82, 153–161. https://doi.org/10.1292/jvms.19-0570

Le Guevel, R., Pakdel, F., 2001. Assessment of oestrogenic potency of chemicals used as growth promoter by in-vitro methods. Hum. Reprod. 16, 1030–1036. https://doi.org/10.1093/humrep/16.5.1030

Li, C.Y., Basit, A., Gupta, A., Gáborik, Z., Kis, E., Prasad, B., 2019. Major glucuronide metabolites of testosterone are primarily transported by MRP2 and MRP3 in human liver, intestine and kidney. J. Steroid Biochem. Mol. Biol. 191, 105350. https://doi.org/10.1016/j.jsbmb.2019.03.027

Lu, Q., Sui, M., Luo, Y.-W., Luo, J.-Y., Yang, M.-H., 2022. Further insight into the potential toxicity of zearalenone-14-glucoside based on toxicokinetics, tissue distribution, transformation, and excretion in rats. Ecotoxicol. Environ. Saf. 246, 114184. https://doi.org/10.1016/j.ecoenv.2022.114184

Malekinejad, H., Maas-Bakker, R., Fink-Gremmels, J., 2006. Species differences in the hepatic biotransformation of zearalenone. Vet. J. 172, 96–102. https://doi.org/10.1016/j.tvjl.2005.03.004

Mallis, L.M., Sarkahian, A.B., Harris, H.A., Zhang, M.-Y., McConnell, O.J., 2003. Determination of rat oral bioavailability of soy-derived phytoestrogens using an automated on-column extraction procedure and electrospray tandem mass spectrometry. J. Chromatogr. B 796, 71–86. https://doi.org/10.1016/j.jchromb.2003.08.003

McKeon, H.P., Schepens, M.A.A., Van Den Brand, A.D., De Jong, M.H., Van Gelder, M.M.H.J., Hesselink, M.L., Sopel, M.M., Mengelers, M.J.B., 2024. Assessment of Mycotoxin

Exposure and Associated Risk in Pregnant Dutch Women: The Human Biomonitoring Approach. Toxins 16, 278. https://doi.org/10.3390/toxins16060278

Mendez-Catala, D.M., Spenkelink, A., Rietjens, I.M.C.M., Beekmann, K., 2020. An in vitromodel to quantify interspecies differences in kinetics for intestinal microbial bioactivation and detoxification of zearalenone. Toxicol. Rep. 7, 938–946. https://doi.org/10.1016/j.toxrep.2020.07.010

Mendez-Catala, D.M., Wang, Q., Rietjens, I.M.C.M., 2021. PBK Model-Based Prediction of Intestinal Microbial and Host Metabolism of Zearalenone and Consequences for its Estrogenicity. Mol. Nutr. Food Res. 65, 2100443. https://doi.org/10.1002/mnfr.202100443

Migdalof, B.H., Dugger, H.A., Heider, J.G., Coombs, R.A., Terry, M.K., 1983. Biotransformation of zeranol: disposition and metabolism in the female rat, rabbit, dog, monkey and man. Xenobiotica 13, 209–221. https://doi.org/10.3109/00498258309052257

Miners, J.O., Rowland, A., Novak, J.J., Lapham, K., Goosen, T.C., 2021. Evidence-based strategies for the characterisation of human drug and chemical glucuronidation in vitro and UDP-glucuronosyltransferase reaction phenotyping. Pharmacol. Ther. 218, 107689. https://doi.org/10.1016/j.pharmthera.2020.107689

Minervini, F., Giannoccaro, A., Cavallini, A., Visconti, A., 2005. Investigations on cellular proliferation induced by zearalenone and its derivatives in relation to the estrogenic parameters. Toxicol. Lett. 159, 272–283. https://doi.org/10.1016/j.toxlet.2005.05.017

Molina-Molina, J.-M., Real, M., Jimenez-Diaz, I., Belhassen, H., Hedhili, A., Torné, P., Fernández, M.F., Olea, N., 2014. Assessment of estrogenic and anti-androgenic activities of the mycotoxin zearalenone and its metabolites using in vitro receptor-specific bioassays. Food Chem. Toxicol. 74, 233–239. https://doi.org/10.1016/j.fct.2014.10.008

Peters, S.A., Jones, C.R., Ungell, A.-L., Hatley, O.J.D., 2016. Predicting Drug Extraction in the Human Gut Wall: Assessing Contributions from Drug Metabolizing Enzymes and Transporter Proteins using Preclinical Models. Clin. Pharmacokinet. 55, 673–696. https://doi.org/10.1007/s40262-015-0351-6

Pfeiffer, E., Hildebrand, A., Mikula, H., Metzler, M., 2010. Glucuronidation of zearalenone, zeranol and four metabolites in vitro: formation of glucuronides by various microsomes and human UDP-glucuronosyltransferase isoforms. Mol Nutr Food Res 54, 1468–76. https://doi.org/10.1002/mnfr.200900524

Pfeiffer, E., Kommer, A., Dempe, J.S., Hildebrand, A.A., Metzler, M., 2011. Absorption and metabolism of the mycotoxin zearalenone and the growth promotor zeranol in Caco-2 cells in vitro. Mol. Nutr. Food Res. 55, 560–567. https://doi.org/10.1002/mnfr.201000381

Ramos, A.J., Hernández, E., Plá-Delfina, J.M., Merino, M., 1996. Intestinal absorption of zearalenone and in vitro study of non-nutritive sorbent materials. Int. J. Pharm. 128, 129–137. https://doi.org/10.1016/0378-5173(95)04239-3

Shin, B.S., Hong, S.H., Bulitta, J.B., Hwang, S.W., Kim, H.J., Lee, J.B., Yang, S.D., Kim, J.E., Yoon, H.-S., Kim, D.J., Yoo, S.D., 2009. Disposition, Oral Bioavailability, and Tissue Distribution of Zearalenone in Rats at Various Dose Levels. J. Toxicol. Environ. Health A 72, 1406–1411. https://doi.org/10.1080/15287390903212774

Utsey, K., Gastonguay, M.S., Russell, S., Freling, R., Riggs, M.M., Elmokadem, A., 2020. Quantification of the impact of partition coefficient prediction methods on physiologically based pharmacokinetic model output using a standardized tissue composition. Drug Metab. Dispos. 48, 903–916. https://doi.org/10.1124/dmd.120.090498

Videmann, B., Koraichi, F., Mazallon, M., Lecoeur, S., 2012. Effect of gender, pregnancy and exposure conditions on metabolism and distribution of zearalenone in rats. World Mycotoxin J. 5, 57–69. https://doi.org/10.3920/WMJ2011.1319

Videmann, B., Mazallon, M., Tep, J., Lecoeur, S., 2008. Metabolism and transfer of the mycotoxin zearalenone in human intestinal Caco-2 cells. Food Chem. Toxicol. 46, 3279–3286. https://doi.org/10.1016/j.fct.2008.07.011